immunoprophylaxis of severe acute respiratory syndrome by an animal study, epitope mapping, and analysis of spike variants. *J Virol* **79:** 5900–6.
10. Matsuyama S., Ujike M., Morikawa S., Tashiro M., Taguchi F. (2005) Protease-mediated enhancement of severe acute respiratory syndrome coronavirus infection. *Proc Natl Acad Sci USA* **102:** 12543–7.
11. Ami Y., Nagata N., Shirato K., Watanabe R., Iwata N., Nakagaki K. *et al.* (2008) Co-infection of respiratory bacterium with severe acute respiratory syndrome coronavirus induces an exacerbated pneumonia in mice. *Microbiol Immunol* **52:** 118–27.
12. Tsunetsugu-Yokota Y., Ato M., Takahashi Y., Hashimoto S., Kaji T., Kuraoka M. *et al.* (2007) Formalin-treated UV-inactivated SARS coronavirus vaccine retains its immunogenicity and promotes Th2-type immune responses. *Jpn J Infect Dis* **60:** 106–12.
13. Ishii K., Hasegawa H., Nagata N., Mizutani T., Morikawa S., Suzuki T. *et al.* (2006) Induction of protective immunity against severe acute respiratory syndrome coronavirus (SARS-CoV) infection using highly attenuated recombinant vaccinia virus DIs. *Virology* **351:** 368–80.
14. Takasuka N., Fujii H., Takahashi Y., Kasai M., Morikawa S., Itamura S. *et al.* (2004) A subcutaneously injected UV-inactivated SARS coronavirus vaccine elicits systemic humoral immunity in mice. *Int Immunol* **16:** 1423–30.
15. Fukushi S., Mizutani T., Saijo M., Kurane I., Taguchi F., Tashiro M. *et al.* (2006) Evaluation of a novel vesicular stomatitis virus pseudotype-based assay for detection of neutralizing antibody responses to SARS-CoV. *J Med Virol* **78:** 1509–12.
16. Nagata N., Iwata N., Hasegawa H., Fukushi S., Yokoyama M., Harashima A. *et al.* (2007) Participation of both host and virus factors in induction of severe acute respiratory syndrome (SARS) in F344 rats infected with SARS coronavirus. *J Virol* **81:** 1848–57.
17. Ohnishi K., Sakaguchi M., Kaji T., Akagawa K., Taniyama T., Kasai M. *et al.* (2005) Immunological detection of severe acute respiratory syndrome coronavirus by monoclonal antibodies. *Jpn J Infect Dis* **58:** 88–94.
18. Mitsuki Y.Y., Ohnishi K., Takagi H., Oshima M., Yamamoto T., Mizukoshi F. *et al.* (2008) A single amino acid substitution in the S1 and S2 Spike protein domains determines the neutralization escape phenotype of SARS-CoV. *Microbes Infect* **10:** 908–15.
19. Wong V.W., Dai D., Wu A.K., Sung J.J. (2003) Treatment of severe acute respiratory syndrome with convalescent plasma. *Hong Kong Med J* **9:** 199–201.
20. Subbarao K., McAuliffe J., Vogel L., Fahle G., Fischer S., Tatti K. *et al.* (2004) Prior infection and passive transfer of neutralizing antibody prevent replication of severe acute respiratory syndrome coronavirus in the respiratory tract of mice. *J Virol* **78:** 3572–7.
21. Sui J., Li W., Murakami A., Tamin A., Matthews L.J., Wong S.K. *et al.* (2004) Potent neutralization of severe acute respiratory syndrome (SARS) coronavirus by a human mAb to S1 protein that blocks receptor association. *Proc Natl Acad Sci USA* **101:** 2536–41.
22. Rockx B., Corti D., Donaldson E., Sheahan T., Stadler K., Lanzavecchia A. *et al.* (2008) Structural basis for potent cross-neutralizing human monoclonal antibody protection against lethal human and zoonotic severe acute respiratory syndrome coronavirus challenge. *J Virol* **82:** 3220–35.
23. Zhu Z., Chakraborti S., He Y., Roberts A., Sheahan T., Xiao X. *et al.* (2007) Potent cross-reactive neutralization of SARS coronavirus isolates by human monoclonal antibodies. *Proc Natl Acad Sci USA* **104:** 12 123–8.
24. McCray P.B., Jr., Pewe L., Wohlford-Lenane C., Hickey M., Manzel L., Shi L. *et al.* (2007) Lethal infection of K18-hACE2 mice infected with severe acute respiratory syndrome coronavirus. *J Virol* **81:** 813–21.
25. Roberts A., Deming D., Paddock C.D., Cheng A., Yount B., Vogel L. *et al.* (2007) A mouse-adapted SARS-coronavirus causes disease and mortality in BALB/c mice. *PLoS Pathog* **3:** e5.
26. Tseng C.T., Huang C., Newman P., Wang N., Narayanan K., Watts D.M. *et al.* (2007) Severe acute respiratory syndrome coronavirus infection of mice transgenic for the human Angiotensin-converting enzyme 2 virus receptor. *J Virol* **81:** 1162–73.

JOURNAL OF VIROLOGY, Dec. 2008, p. 11985–11991 Vol. 82, No. 23
0022-538X/08/$08.00+0 doi:10.1128/JVI.01412-08

Entry from the Cell Surface of Severe Acute Respiratory Syndrome Coronavirus with Cleaved S Protein as Revealed by Pseudotype Virus Bearing Cleaved S Protein▽

Rie Watanabe,[1] Shutoku Matsuyama,[1] Kazuya Shirato,[1] Masami Maejima,[1] Shuetsu Fukushi,[2] Shigeru Morikawa,[2] and Fumihiro Taguchi[1]*

Departments of Virology III[1] and I,[2] National Institute of Infectious Diseases, Murayama Branch, Musashi-Murayama, Tokyo 208-0011, Japan

Received 8 July 2008/Accepted 3 September 2008

Severe acute respiratory syndrome (SARS) coronavirus (SARS-CoV) is known to take an endosomal pathway for cell entry; however, it is thought to enter directly from the cell surface when a receptor-bound virion spike (S) protein is affected by trypsin, which induces cleavage of the S protein and activates its fusion potential. This suggests that SARS-CoV bearing a cleaved form of the S protein can enter cells directly from the cell surface without trypsin treatment. To explore this possibility, we introduced a furin-like cleavage sequence in the S protein at amino acids 798 to 801 and found that the mutated S protein was cleaved and induced cell fusion without trypsin treatment when expressed on the cell surface. Furthermore, a pseudotype virus bearing a cleaved S protein was revealed to infect cells in the presence of a lysosomotropic agent as well as a protease inhibitor, both of which are known to block SARS-CoV infection via an endosome, whereas the infection of pseudotypes with an uncleaved, wild-type S protein was blocked by these agents. A heptad repeat peptide, derived from a SARS-CoV S protein that is known to efficiently block infections from the cell surface, blocked the infection by a pseudotype with a cleaved S protein but not that with an uncleaved S protein. Those results indicate that SARS-CoV with a cleaved S protein is able to enter cells directly from the cell surface and agree with the previous observation of the protease-mediated cell surface entry of SARS-CoV.

A causative agent of the severe acute respiratory syndrome (SARS) that spread worldwide in 2002 to 2003 is a newly identified SARS coronavirus (SARS-CoV) (29). SARS-CoV is an enveloped virus with a positive-sense, single-stranded genome RNA of 29 kilobases (25) and is classified into the group 2 CoVs (34).

SARS-CoV spike (S) protein is a class I fusion glycoprotein having a molecular mass of ca. 200 kDa and is responsible for attachment to its receptor and subsequent entry into cells (6, 35, 40). During the maturation of the SARS-CoV S protein, its cleavage by intracellular protease is not observed (6, 35), which is similar to findings with the S protein of group 1 CoVs, such as human CoV 229E and transmissible gastroenteritis virus (4, 17, 19, 31). However, cleaved S1 and S2 (cl-S) subunits are detected on virions and in cells infected with murine CoV mouse hepatitis virus (MHV) and some other group 2 CoVs (36, 39). Although Bergeron et al. reported that certain proprotein convertases facilitate the processing of SARS-CoV S protein (3), others failed to find any subunits corresponding to S1 and S2 in cells infected with SARS-CoV or transfected with an S protein expression plasmid (27, 32, 35, 39). Uncleaved S proteins of SARS-CoV and others consist of regions that correspond to the S1 and S2 subunits of the MHV S protein. The receptor-binding domain (RBD) of SARS-CoV is located at amino acids 270 to 510 of the S1 subunit (2), making it similar to the RBD of group 1 CoVs (4, 10, 39) but different from that of MHV, which has its RBD in an N-terminal, 330-amino-acid region of the S1 subunit (21). Membrane-anchored S2 subunits of CoVs and corresponding regions in SARS-CoV S protein are structurally similar to the class I fusion proteins of other enveloped viruses (6, 7, 12). However, the fusion peptide that plays a crucial role in virus-to-cell fusion is located at the N terminus of the membrane-anchored subunit in influenza virus and human immunodeficiency virus (HIV), which in SARS-CoV and other CoVs is located in an internal region of the S2 subunit (6, 8, 12, 18, 24, 30, 37).

SARS-CoV was reported to enter target cells by two different pathways, one via an endosome and the other from the cell surface (27, 32, 33). In the endosomal pathway, the virus particle that attached to its receptor, angiotensin-converting enzyme 2 (ACE2) (23), is trafficked into the endosome, and then the S protein is cleaved at amino acid position 678 by an endosomal protease, cathepsin L (CPL), which activates the S protein fusion activity (5). This results in a fusion of the viral envelope and endosome membrane and subsequent internalization of the virus genome into cells (5, 33). On the other hand, the virion S protein attached to cell surface ACE2 is activated for fusion by proteases such as trypsin, which induces cleavage at amino acid position 667 of the S protein, 11 amino acids upstream of the CPL cleavage site (5, 22), which results in the fusion of the virus envelope and plasma membrane and subsequent viral entry from the cell surface (27). Entry from the cell surface is therefore possible only in the presence of proteases that activate the S protein. In both pathways, the

* Corresponding author. Mailing address: Laboratory of Respiratory Viral Infections and SARS, National Institute of Infectious Diseases, Murayama Branch, 4-7-1 Gakuen, Mushai-Murayama, Tokyo 208-0011, Japan. Phone: 81-42-561-0771, ext. 3533. Fax: 81-42-567-5631. E-mail: ftaguchi@nih.go.jp.

▽ Published ahead of print on 10 September 2008.

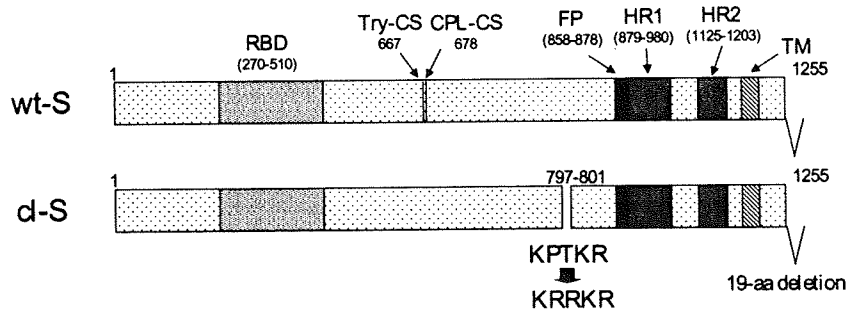

FIG. 1. Schematic illustration of SARS-CoV wt-S protein and its mutant (cl-S). S proteins are shown in the box, in which the RBD, putative fusion peptide (FP), two HRs, and transmembrane region (TM) are indicated. Cleavage sites by trypsin (Try-CS) and CPL (CPL-CS) are also shown. Amino acid positions 798 and 799 are changed into arginine to make the recognition sequence of furin-like protease, KRRKR. Nineteen C-terminal amino acids (aa) are deleted for the efficient pseudotype formation of VSV.

cleavage and fusogenic activation of SARS-CoV S protein are a critical step for virus entry into cells.

The preceding observations led us to postulate that SARS-CoV with cl-S protein that induces cell-to-cell fusion in the absence of proteases is able to enter cells directly from the cell surface, being similar to the cell entry of MHV with cl-S protein (16, 28). To explore this possibility, we have made a cleavage mutant of the SARS-CoV S protein by introducing the recognition sequence of furin-like protease, produced pseudotyped vesicular stomatitis virus (VSV) bearing this S protein, and analyzed whether cl-S protein facilitates direct viral entry from the cell surface.

We have chosen two different sites of S protein to introduce the furin recognition sequence (FRS) (RXR/KR; X indicates any amino acid residue [11]), one at positions 663 to 667 and the other at 798 to 801, since both contain a few endogenous basic amino acids and need not be drastically mutated to introduce FRS. The former corresponds to the site cleaved by trypsin (22) and also to the site of the MHV S protein which is cleaved during biosynthesis (36); however, insertion of FRS in this region failed to produce cleaved and fusogenic S protein in our system, being different from a previous report by Follis et al. (14). Thus, we introduced the FRS into a second region at positions 798 to 801. The mutated S protein was revealed to be fusogenic and was also cleaved by endogenous proteases, most probably by furin. In this study, we have analyzed the relationship of cleavability and fusogenicity of S protein as well as the cell entry pathway of the pseudotype VSV bearing the cl-S protein (VSV/cl-S) with a mutation at amino acid positions 798 to 801.

FRS was introduced at amino acid positions 798 to 801 in SARS-CoV S protein by an overlapping PCR method (14), and the resultant S protein was designated cl-S. Nineteen C-terminal amino acids were deleted for the efficient formation of pseudotype VSV, as described by Fukushi et al. (15). The mutated cDNA, as well as the cDNA for wild-type S (wt-S) protein lacking the 19 C-terminal amino acid residues, was cloned into a pCAG vector, and the nucleotide sequence was confirmed by DNA sequencing using BigDye Terminator version 3.1 and a 3130xl genetic analyzer (Applied Biosystems, Foster, CA). Figure 1 shows a schematic illustration of these S proteins.

The expression plasmids pCAG/cl-S and pCAG/wt-S, encoding SARS-CoV cl-S and SARS-CoV wt-S proteins, respectively, were transfected into HeLa cells and HeLa-ACE2 cells by using FuGENE6 (Roche Diagnostics, Mannheim, Germany), and those cells were incubated for 48 h after transfection. HeLa-ACE2 cells that constitutively express ACE2 were established from HeLa cells, following the transfection of a plasmid to express ACE2. The cells cultured for 48 h were also treated with 20 μg/ml of trypsin at room temperature for 5 min and further cultured at 37°C for 2 h to check cell fusion. As shown in Fig. 2A, large syncytia were visible on the HeLa-ACE2 cells transfected with pCAG/cl-S without trypsin treatment, whereas there was no apparent syncytium formation on the cells transfected with pCAG/wt-S. Treatment with trypsin induced fusion of the cells expressing wt-S protein. On the other hand, neither of those S proteins could induce cell-to-cell fusion on HeLa cells, even when they were treated by trypsin. These results strongly indicated that the cleavage of the S protein at amino acid position 798 converted its protease-dependent fusion phenotype to a protease-independent one and that ACE2 is crucial for the induction of cell-to-cell fusion. We then confirmed the cleavage of the S protein in those cells by Western blot analysis using anti-S2 rabbit serum no. 557 (Imgenex, San Diego, CA). Cells treated or untreated with trypsin were lysed with lysis buffer (10% glycerol, 1% Triton X-100, 135 mM NaCl) 5 min after treatment, and cell lysates were subjected to Western blot analysis. As shown in Fig. 2B, an S2 fragment with a molecular mass of 70 kDa was detected in the cell lysates prepared from pCAG/cl-S-transfected HeLa-ACE2 cells but not in the lysate of cells transfected with pCAG/wt-S (Fig. 2B). The 70-kDa protein found in cells transfected with pCAG/cl-S seems likely to correspond to the S2 fragment cleaved at the site where mutations recognized by furin-like protease are inserted, since its putative size was calculated to be approximately 68 kDa. It was also found that a proportion of cl-S protein expressed on HeLa-ACE2 cells was cleaved into a 100-kDa protein from a 240-kDa uncleaved form of S protein by trypsin treatment. The appearance of this 100-kDa protein in the lysates of trypsin-treated cells could result from the cleavage at amino acid position 667 (22), consistent with previous reports, and this subunit has been suggested to be involved in an S protein-mediated fusion (27, 32). Accordingly, cell fusion induction by trypsin of wt-S protein-expressing cells shown in the present study may be due to the

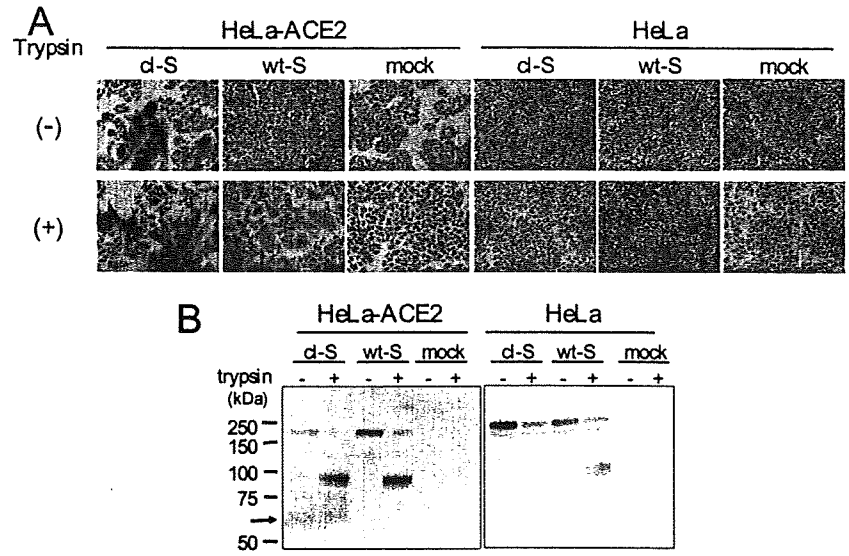

FIG. 2. Fusion formation and cleavability of cl-S and wt-S proteins transiently expressed in cells with and without ACE2 expression. (A) HeLa-ACE2 and HeLa cells were transfected with pCAG plasmid containing cl-S or wt-S proteins or were mock transfected (mock) by using FuGENE6 and were incubated for 48 h. Then, cells were treated (+) or untreated (−) with 20 μg/ml of trypsin at room temperature for 5 min and further incubated in DMEM containing 5% FBS at 37°C for 2 h. Then, formalin-fixed cells were stained with crystal violet. (B) Expression of the S2 subunit in cells transfected with S protein expression plasmids. Cells treated as described above were lysed before (−) or after (+) trypsin treatment and analyzed by Western blotting using anti-S2 antiserum (no. 557; Imgenex). Arrow indicates the cl-S2 subunit, as judged by its molecular size.

presence of 100 kDa of S2 protein (Fig. 2B). Also, the slightly elevated syncytium formation by trypsin treatment of the cells expressing cl-S protein 48 h after transfection (Fig. 2A, compare HeLa-ACE2 cells expressing cl-S protein and treated with trypsin to similar cells without trypsin treatment) could be attributed to a 100-kDa protein that arose after trypsin treatment. When cl-S protein was expressed in HeLa cells deleting ACE2, cleavage products were not detected, resulting in the absence of cell-to-cell fusion. Treatment of HeLa cells expressing wt-S or cl-S proteins with trypsin facilitated the cleavage of 240 kDa into 100 kDa, which was similar to the type of cleavage observed in HeLa-ACE2 cells; however, no fusion was detected, which indicated to us that ACE2 is crucial for the induction of cell-to-cell fusion. These results suggest that cl-S protein with a 70-kDa S2 subunit can induce fusion in a protease-independent manner.

Recently, Bosch et al. reported that SARS-CoV S proteins were cleaved by CPL at amino acid 678, resulting in a ca. 70-kDa S2 subunit (5), while the cl-S protein cleaved at position 798 shown in this study also resulted in a 60- to 70-kDa S2 subunit, even if the cleavage site was about 120 amino acids apart. This coincidence of the molecular mass of two different S2 subunits could come from the difference of S protein structure used in each experiment. We used full-length S, deleting 19 C-terminal amino acids, while S protein utilized by Bosch et al. was the soluble form of S protein, deleting transmembrane, and cytoplasmic domains consisted of ca. 60 amino acids (5). The full-length S2 subunit cleaved by CPL in SARS-CoV-infected cells would be ca. 100 kDa, similar to the S2 subunit cleaved by trypsin, because cleavage sites of those two proteases are closely located and only 11 amino acids apart (5, 22).

To evaluate the significance of the cleavage of the S protein to the entry pathway of SARS-CoV, pseudotyped VSV/cl-S or VSV/wt-S protein was produced as described previously (15, 26). In brief, expression plasmids for cl-S or wt-S protein were transfected to 293T cells, and those cells were infected with VSV bearing the glycoprotein (G), VSVΔG*G/SEAP, or VSVΔG*G/GFP, at 36 h after transfection. VSVΔG*G/SEAP and VSVΔG*G/GFP have a secretary alkaline phosphatase (SEAP) gene and the green fluorescence protein (GFP) gene in place of the VSV viral G gene, respectively. To confirm the S protein on the pseudotype viruses released in the culture supernatants, the supernatant was collected at 24 h after infection, and pseudotyped VSV was concentrated by ultracentrifugation at 45,000 rpm for 2 h at 4°C using an SW50.1 rotor (Beckman, Fullerton, CA). The resultant pellets were dissolved in phosphate-buffered saline, pH 7.2, and analyzed by Western blotting after sodium dodecyl sulfate-polyacrylamide gel electrophoresis. To detect S1 and S2 subunits, we used anti-S1 no. 20 (epitope, 20 to 35) and anti-S2 no. 1125 (epitope, 1125 to 1140) produced by the immunization of a chicken with synthetic peptides. As shown in Fig. 3A, a ca. 150-kDa protein and a 240-kDa protein was detected on pseudotyped VSV/cl-S by anti-S1 antibodies, while a ca. 70-kDa as well as a 240-kDa protein was detected by S2 subunit-specific antibodies. On the other hand, only the 240-kDa protein was seen on the pseudotype VSV/wt-S by both antibodies. The 150-kDa and 70-kDa proteins detected on pseudotype VSV/cl-S by anti-S1 and S2 antibodies, respectively, were thought to be cleavage products from their antigenicity and sizes. These results indicate that VSV pseudotypes with cl-S or wt-S protein were successfully formed, although the former is a mixture of pseudotypes with cl-S and uncleaved S protein (Fig. 3A). To obtain a preparation containing a higher proportion of pseudotype with cl-S protein, we expressed furin and ACE2 in 293T cells transfected with pCAG/cl-S because the production of a 70-kDa S2 subunit during synthesis was observed only in the presence of ACE2 (Fig. 2B). However, this

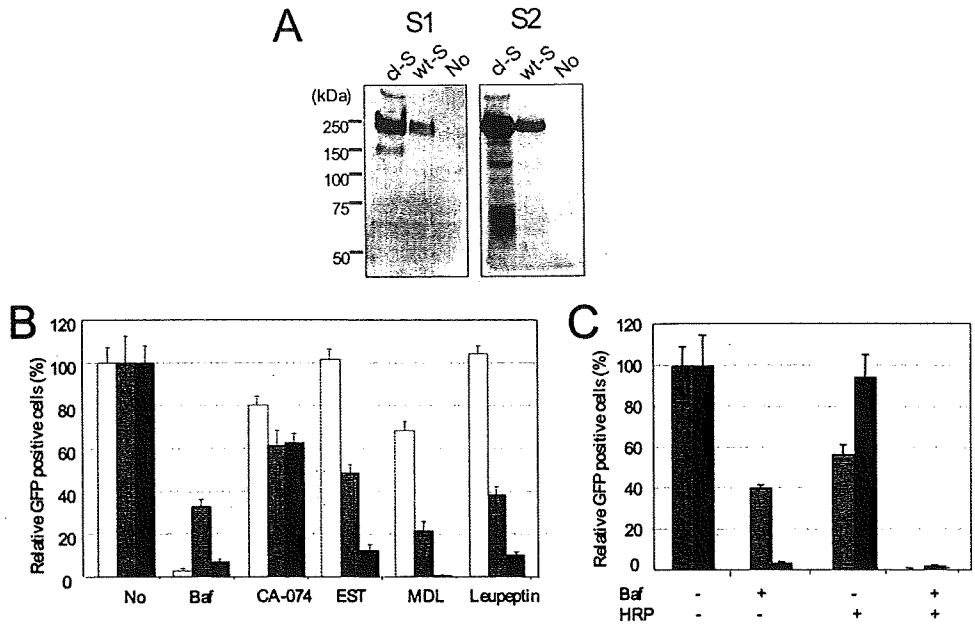

FIG. 3. Analysis using pseudotype VSV/cl-S or VSV/wt-S protein. (A) The incorporation of S protein into the pseudotype VSV. Pseudotype VSV was prepared by transfection of expression plasmids harboring the cl-S gene, the wt-S gene, or no gene and infection of VSVΔG*G. The pseudotypes in the culture fluids were concentrated by spinning at 45,000 rpm for 2 h using the SW50.1 rotor of a Beckman ultracentrifuge. The resultant pellets were dissolved in lysis buffer and analyzed by Western blot analysis using chicken antisera against S1 and S2 subunits (anti-S1 no. 20 and anti-S2 no. 1125, respectively). (B) Effect of Baf, protease inhibitors CA-074, EST, MDL, or leupeptin on the infection of VSV/G (white column), VSV/cl-S (gray column), or VSV/wt-S (black column) protein. HeLa-ACE2 cells prepared in 96-well plates were treated with those reagents at 37°C for 1 h, and ca. 500 PFU/50 μl of pseudotype VSVs were challenged. The infection was evaluated by measuring the number of GFP gene-positive cells in the wells at 24 h after infection as determined by Keyence fluorescence microscopy. (C) Blockade of pseudotype VSV infection by HRP. HeLa-ACE2 cells prepared in 96-well plates were treated with either Baf and/or HRP (5 μM) for 30 min at 37°C, infected with pseudotype VSVs that express GFP, adsorbed at 4°C for 1 h, and then incubated in the presence of Baf and/or HRP at 37°C for 24 h. The infection was evaluated as described above.

treatment did not increase the amount of cl-S proteins on the pseudotypes (data not shown).

We then examined the cell entry pathway of the viruses with cl-S and uncleaved SARS-CoV S proteins by using the above-mentioned preparation of two different pseudotype VSVs. To see whether the virus with cl-S protein bypassed an endosomal pathway, we evaluated the effect on the virus infection of the lysosomotropic agent bafilomycin A1 (Baf) in HeLa-ACE2 cells. The cells seeded at a concentration of 2×10^4 cells per well in a 96-well culture plate (Smilon, Tokyo, Japan) the day before infection were incubated in Dulbecco's minimum essential medium (DMEM; Nissui, Tokyo, Japan) containing 5% fetal bovine serum (FBS; Sigma) and 100 nM Baf (Sigma) for 1 h at 37°C before infection. Then, ca. 500 infectious units of GFP gene-positive pseudotype VSV/cl-S, VSV/wt-S, or VSV/G was inoculated and incubated at 37°C for 1 h. Those cells were further incubated for 23 h in DMEM plus 5% FBS containing 100 nM Baf. GFP gene-positive cells were photographed by Keyence fluorescence microscopy (Keyence Corporation, Osaka, Japan), and cell numbers were calculated by using the image measurement and analyzing software VH-H1A5 version 2.6 (Keyence). As shown in Fig. 3B, the infection by VSV/wt-S was reduced by more than 90% by Baf treatment, similar to the suppression seen with VSV/G infection, which takes the endosomal pathway, while the suppression of VSV/cl-S infection was ca. 60%. This finding indicated that a proportion of VSV/cl-S infection was not affected by low pH in the endosome, which suggested that pseudotypes with cl-S protein do not take the endosomal pathway. About 60% of the reduction in infection of VSV/cl-S could be accounted for by the pseudotypes bearing uncleaved S protein, which was contaminated in the pseudotype with cl-S protein, as shown in Fig. 3A. We then examined whether the infection of pseudotypes is affected by treatment with protease inhibitors in a manner similar to that seen with SARS-CoV infection (33). Cells were treated with DMEM containing 100 μM of CPL inhibitor MDL (Sigma), 50 μM of CPL inhibitor EST (Carbiochem, Darmstadt, Germany), 200 μM of cathepsin B inhibitor CA-074 (Sigma), or 50 μM of cysteine protease inhibitor leupeptin (Roche Diagnostics) in a manner similar to that with Baf treatment and then infected with pseudotype viruses. GFP gene-positive cells were calculated as described above. Infection with the pseudotype bearing wt-S protein was heavily blocked by MDL, EST, and leupeptin, while pseudotypes with cl-S protein infection were partially inhibited (Fig. 3B), which indicated that VSV/wt-S requires CPL for its infection, while VSV/cl-S does not require CPL. A fraction of pseudotypes with cl-S protein sensitive to protease inhibitor treatment is also explained by the contamination of a pseudotype bearing uncleaved S protein. These results collectively suggest that VSV/cl-S could bypass the endosomal pathway in which S protein activation was induced by CPL and, thus, that VSV/cl-S most likely enters target cells directly from the cell surface.

To further confirm that VSV/cl-S enters directly from the cell surface, we utilized a heptad repeat peptide (HRP) that was recently shown to efficiently block SARS-CoV infection from the cell surface but not the infection via the endosomal pathway (38). HeLa-ACE2 cells were treated with a final concentration of 100 nM of Baf and/or 5 μM of HRP-SR9, a peptide of 35 amino acids that corresponds to positions 1151 to 1185 of the SARS-CoV S protein (38), for 30 min at 37°C. Then, pseudotype VSVs were allowed to attach to cells at 4°C for 1 h in the presence of those agents. Then, cells were cultured at 37°C for 24 h in their presence, and the number of GFP gene-positive cells was calculated. As shown in Fig. 3C, Baf treatment alone thoroughly blocked infection with VSV/wt-S and that of VSV/cl-S by 40%, which seemed to indicate that some population of VSV/cl-S could bypass the endosomal pathway as shown in Fig. 3B. When treated with HRP, infection with VSV/wt-S was not at all blocked, which was similar to the results obtained previously (38), while infection with VSV/cl-S was partially blocked. The fraction of virus inhibited by HRP treatment may represent the VSV/cl-S. Furthermore, when treated with Baf and HRP, infection with VSV/cl-S was blocked almost completely, which suggested that the infection of Baf-resistant VSV/cl-S was blocked by HRP treatment. Another HRP (SR9EK1), previously shown to not prevent cell surface entry (38), failed to inhibit VSV/cl-S infection (data not shown). These results suggest that VSV/cl-S enters directly from the cell surface.

Two different pathways for cell entry are known for enveloped viruses, one from the cell surface and the other via an endosome (12). HIV and influenza virus are representative of the former and latter, respectively. Following binding to its receptor/coreceptor, gp160 of HIV is fusogenically activated, and fusion of the viral envelope and plasma membrane takes place, which facilitates the entry of the virus directly from the cell surface. In contrast, activation by hemagglutinin of influenza virus requires a low pH environment in the endosome to which virions are trafficked, following binding to its receptor. A strain of murine CoV, MHV-JHM, is believed to enter cells from the cell surface (16), while another strain, namely, MHV-A59, uses an endosomal pathway for entry due to its similarity to the entry mechanism of influenza virus (13). Although SARS-CoV takes an endosomal pathway, the molecular mechanism of entry is quite different from that of MHV-A59 or influenza virus. SARS-CoV S protein activation is not induced under a low pH environment but by proteolytic cleavage by CPL in the endosome that provides a low pH environment, which is optimal for CPL activity (5, 33). This entry mechanism is unique, though Ebola virus was initially shown to enter into cells in a similar fashion (9). Based on these molecular events of SARS-CoV infection, it can be postulated that SARS-CoV bearing a cl-S protein with fusion activity is able to enter cells directly from the cell surface, such as HIV and MHV-JHM do. The present study showed that cl-S protein along with the cell fusion activity of SARS-CoV facilitated viral entry into cells directly from the cell surface and strengthened the premise concerning the cell entry mechanism of SARS-CoV, as proposed by previous findings from different laboratories (27, 32, 33).

In the present study, we designed a mutant S protein to be cleaved during its maturation at the 798 amino acid position by inserting a recognition site for the furin-like protease. The detection of a 70-kDa fragment by anti-S2 antibody in Western blot analysis suggests that cleavage takes place at an expected position. Follis et al. produced a mutant with a cleavage site at amino acid position 667 (14). An S2 subunit of this mutant S protein was shown to be ca. 100 kDa and fusogenic, although insertion of extra amino acids in a newly appearing cleavage site is required for enhanced fusogenicity (14). We also produced and expressed the S protein without an extra amino acid insertion, as reported by Follis et al. (14), although it failed to induce cell-to-cell fusion in the absence of trypsin but successfully induced fusion when treated with trypsin, similar to the wt-S protein (data not shown). In our system, S protein with a cleavage site at amino acid 798 is only an S protein competent in the induction of cell-to-cell fusion without trypsin treatment.

It is clear that there is no stringency in the cleavage site of the SARS-CoV S protein for the fusion activity. Cleavage of the S protein by trypsin and CPL resulted in the fusion activity (5, 27, 32), even if the cleavage site was slightly different (5, 22). Also, our present study showed that cleavage at 120 amino acids downstream compared with the sites of trypsin and CPL conferred the fusion activity to the S2 protein. This is a unique feature of CoV S protein that was not found in the envelope protein of other viruses having a class I fusion protein, like HIV or influenza virus.

The finding that cl-S2 cleaved at position 798 has fusion activity implies that this molecule has a fusion peptide together with two different heptide repeats (HRs), motifs critical for fusion activity of class I fusion protein of the virus. This suggests that the fusion peptide on SARS-CoV S protein would locate downstream of amino acid position 798. Although there are controversial reports on the localization of a fusion peptide in SARS-CoV S protein, present study suggests that the fusion peptide locates immediately upstream of the HR1 (18) rather than in the 770 to 788 region (30), because this region is located outside the fusogenic 70-kDa S2 subunit produced by cl-S protein expression.

We reported that SARS-CoV infection was enhanced in cultured cells in the presence of proteases, such as trypsin and elastase, and that this enhancement was facilitated by virus entry from the cell surface (27). Elastase is a major protease produced by neutrophils during lung inflammation and may be relevant to the high growth of SARS-CoV in the lung, a major target organ (20). Based on these findings, we have established an exacerbated fatal pneumonia of mice with high pathogenic similarity to human SARS by the coinfection of SARS-CoV and nonpathogenic respiratory bacteria that stimulates elastase secretion (1). Severe pneumonia of mice was attributed to an enhanced SARS-CoV infection in the lung that could be facilitated by the elastase (1). We have not evaluated yet whether this enhanced infection is due to the cell surface infection. If this is the case, HRP may be a good candidate for a therapeutic tool, since HRP efficiently blocks SARS-CoV infection from the cell surface, as shown in the present and previous studies (38).

Most MHV strains induce cell-to-cell fusion in infected cells, yet a highly hepatopathogenic strain, MHV-2, fails to induce fusion (41). MHV-2 shares a common feature with SARS-CoV in terms of its S protein. MHV-2 was revealed to enter cells in

a fashion highly similar to that of SARS-CoV, which is dependent on the proteases in the endosomal compartment having a low pH environment (28). A mutant virus with fusogenic S protein was isolated from wild-type MHV-2 bearing uncleaved S protein, although isolation was extremely low in efficiency, ca. 1 mutant out of half a million to 1 million (41). This could suggest the possibility that SARS-CoV with fusogenic cl-S protein exists among a large number of viruses with uncleaved S protein. It is of interest to see the effects of SARS-CoV with a cl-S protein in terms of cell entry mechanisms as well as in pathogenesis for animals.

We thank Miyuki Kawase for her excellent technical assistance, Makoto Ujike for helpful discussions, and Hiroki Nishikawa and Nobutaka Fujii for providing HRP. We also thank Sarah Connolly for editing the manuscripts and for valuable comments.

This work was supported by grants from the Ministry of Education, Culture, Science, and Technology and from the Ministry of Health, Labor, and Welfare.

REFERENCES

1. **Ami, Y., N. Nagata, K. Shirato, R. Watanabe, N. Iwata, K. Nakagaki, S. Fukushi, M. Saijo, S. Morikawa, and F. Taguchi.** 2008. Co-infection of respiratory bacterium with SARS coronavirus induces an exacerbated pneumonia in mice. Microbiol. Immunol. **52:**118–127.
2. **Babcock, G. J., D. J. Esshaki, W. D. Thomas, Jr., and D. M. Ambrosino.** 2004. Amino acids 270 to 510 of the severe acute respiratory syndrome coronavirus spike protein are required for interaction with receptor. J. Virol. **78:**4552–4560.
3. **Bergeron, E., M. J. Vincent, L. Wickham, J. Hamelin, A. Basak, S. T. Nichol, M. Chretien, and N. G. Seidah.** 2005. Implication of proprotein convertases in the processing and spread of severe acute respiratory syndrome coronavirus. Biochem. Biophys. Res. Commun. **326:**554–563.
4. **Bonavia, A., B. D. Zelus, D. E. Wentworth, P. J. Talbot, and K. V. Holmes.** 2003. Identification of a receptor-binding domain of the spike glycoprotein of human coronavirus HCoV-229E. J. Virol. **77:**2530–2538.
5. **Bosch, B. J., W. Bartelink, and P. J. M. Rottier.** 2008. Cathepsin L functionally cleaves the SARS-CoV class-I fusion protein upstream of rather than adjacent to the fusion peptide. J. Virol. **82:**8887–8890.
6. **Bosch, B. J., B. E. Martina, R. van der Zee, J. Lepault, B. J. Haijema, C. Versluis, A. J. Heck, R. de Groot, A. D. Osterhaus, and P. J. Rottier.** 2004. Severe acute respiratory syndrome coronavirus (SARS-CoV) infection inhibition using spike protein heptad repeat-derived peptides. Proc. Natl. Acad. Sci. USA **101:**8455–8460.
7. **Bosch, B. J., R. van der Zee, C. A. de Haan, and P. J. Rottier.** 2003. The coronavirus spike protein is a class I virus fusion protein: structural and functional characterization of the fusion core complex. J. Virol. **77:**8801–8811.
8. **Chan, D. C., and P. S. Kim.** 1998. HIV entry and its inhibition. Cell **93:**681–684.
9. **Chandran, K., N. J. Sullivan, U. Felbor, S. P. Whelan, and J. M. Cunningham.** 2005. Endosomal proteolysis of the Ebola virus glycoprotein is necessary for infection. Science **308:**1643–1645.
10. **Delmas, B., J. Gelfi, E. Kut, H. Sjostrom, O. Noren, and H. Laude.** 1994. Determinants essential for the transmissible gastroenteritis virus-receptor interaction reside within a domain of aminopeptidase-N that is distinct from the enzymatic site. J. Virol. **68:**5216–5224.
11. **Duckert, P., S. Brunak, and N. Blom.** 2004. Prediction of proprotein convertase cleavage sites. Protein Eng. Des. Sel. **17:**107–112.
12. **Eckert, D. M., and P. S. Kim.** 2001. Mechanisms of viral membrane fusion and its inhibition. Annu. Rev. Biochem. **70:**777–810.
13. **Eifart, P., K. Ludwig, C. Bottcher, C. A. de Haan, P. J. Rottier, T. Korte, and A. Herrmann.** 2007. Role of endocytosis and low pH in murine hepatitis virus strain A59 cell entry. J. Virol. **81:**10758–10768.
14. **Follis, K. E., J. York, and J. H. Nunberg.** 2006. Furin cleavage of the SARS coronavirus spike glycoprotein enhances cell-cell fusion but does not affect virion entry. Virology **350:**358–369.
15. **Fukushi, S., T. Mizutani, M. Saijo, S. Matsuyama, N. Miyajima, F. Taguchi, S. Itamura, I. Kurane, and S. Morikawa.** 2005. Vesicular stomatitis virus pseudotyped with severe acute respiratory syndrome coronavirus spike protein. J. Gen. Virol. **86:**2269–2274.
16. **Gallagher, T. M., C. Escarmis, and M. J. Buchmeier.** 1991. Alteration of the pH dependence of coronavirus-induced cell fusion: effect of mutations in the spike glycoprotein. J. Virol. **65:**1916–1928.
17. **Garwes, D. J., and D. H. Pocock.** 1975. The polypeptide structure of transmissible gastroenteritis virus. J. Gen. Virol. **29:**25–34.
18. **Guillén, J., A. J. Perez-Berna, M. R. Moreno, and J. Villalain.** 2005. Identification of the membrane-active regions of the severe acute respiratory syndrome coronavirus spike membrane glycoprotein using a 16/18-mer peptide scan: implications for the viral fusion mechanism. J. Virol. **79:**1743–1752.
19. **Hofmann, H., G. Simmons, A. J. Rennekamp, C. Chaipan, T. Gramberg, E. Heck, M. Geier, A. Wegele, A. Marzi, P. Bates, and S. Pöhlmann.** 2006. Highly conserved regions within the spike proteins of human coronaviruses 229E and NL63 determine recognition of their respective cellular receptors. J. Virol. **80:**8639–8652.
20. **Kawabata, K., T. Hagio, and S. Matsuoka.** 2002. The role of neutrophil elastase in acute lung injury. Eur. J. Pharmacol. **451:**1–10.
21. **Kubo, H., Y. K. Yamada, and F. Taguchi.** 1994. Localization of neutralizing epitopes and the receptor-binding site within the amino-terminal 330 amino acids of the murine coronavirus spike protein. J. Virol. **68:**5403–5410.
22. **Li, F., M. Berardi, W. Li, M. Farzan, P. R. Dormitzer, and S. C. Harrison.** 2006. Conformational states of the severe acute respiratory syndrome coronavirus spike protein ectodomain. J. Virol. **80:**6794–6800.
23. **Li, W., M. J. Moore, N. Vasilieva, J. Sui, S. K. Wong, M. A. Berne, M. Somasundaran, J. L. Sullivan, K. Luzuriaga, T. C. Greenough, H. Choe, and M. Farzan.** 2003. Angiotensin-converting enzyme 2 is a functional receptor for the SARS coronavirus. Nature **426:**450–454.
24. **Luo, Z., and S. R. Weiss.** 1998. Roles in cell-to-cell fusion of two conserved hydrophobic regions in the murine coronavirus spike protein. Virology **244:**483–494.
25. **Marra, M. A., S. J. Jones, C. R. Astell, R. A. Holt, A. Brooks-Wilson, Y. S. Butterfield, J. Khattra, J. K. Asano, S. A. Barber, S. Y. Chan, A. Cloutier, S. M. Coughlin, D. Freeman, N. Girn, O. L. Griffith, S. R. Leach, M. Mayo, H. McDonald, S. B. Montgomery, P. K. Pandoh, A. S. Petrescu, A. G. Robertson, J. E. Schein, A. Siddiqui, D. E. Smailus, J. M. Stott, G. S. Yang, F. Plummer, A. Andonov, H. Artsob, N. Bastien, K. Bernard, T. F. Booth, D. Bowness, M. Czub, M. Drebot, L. Fernando, R. Flick, M. Garbutt, M. Gray, A. Grolla, S. Jones, H. Feldmann, A. Meyers, A. Kabani, Y. Li, S. Normand, U. Stroher, G. A. Tipples, S. Tyler, R. Vogrig, D. Ward, B. Watson, R. C. Brunham, M. Krajden, M. Petric, D. M. Skowronski, C. Upton, and R. L. Roper.** 2003. The genome sequence of the SARS-associated coronavirus. Science **300:**1399–1404.
26. **Matsuura, Y., H. Tani, K. Suzuki, T. Kimura-Someya, R. Suzuki, H. Aizaki, K. Ishii, K. Moriishi, C. S. Robison, M. A. Whitt, and T. Miyamura.** 2001. Characterization of pseudotype VSV possessing HCV envelope proteins. Virology **286:**263–275.
27. **Matsuyama, S., M. Ujike, S. Morikawa, M. Tashiro, and F. Taguchi.** 2005. Protease-mediated enhancement of severe acute respiratory syndrome coronavirus infection. Proc. Natl. Acad. Sci. USA **102:**12543–12547.
28. **Qiu, Z., S. T. Hingley, G. Simmons, C. Yu, J. Das Sarma, P. Bates, and S. R. Weiss.** 2006. Endosomal proteolysis by cathepsins is necessary for murine coronavirus mouse hepatitis virus type 2 spike-mediated entry. J. Virol. **80:**5768–5776.
29. **Rota, P. A., M. S. Oberste, S. S. Monroe, W. A. Nix, R. Campagnoli, J. P. Icenogle, S. Penaranda, B. Bankamp, K. Maher, M. H. Chen, S. Tong, A. Tamin, L. Lowe, M. Frace, J. L. DeRisi, Q. Chen, D. Wang, D. D. Erdman, T. C. Peret, C. Burns, T. G. Ksiazek, P. E. Rollin, A. Sanchez, S. Liffick, B. Holloway, J. Limor, K. McCaustland, M. Olsen-Rasmussen, R. Fouchier, S. Gunther, A. D. Osterhaus, C. Drosten, M. A. Pallansch, L. J. Anderson, and W. J. Bellini.** 2003. Characterization of a novel coronavirus associated with severe acute respiratory syndrome. Science **300:**1394–1399.
30. **Sainz, B., Jr., J. M. Rausch, W. R. Gallaher, R. F. Garry, and W. C. Wimley.** 2005. Identification and characterization of the putative fusion peptide of the severe acute respiratory syndrome-associated coronavirus spike protein. J. Virol. **79:**7195–7206.
31. **Schmidt, O. W., and G. E. Kenny.** 1982. Polypeptide and functions of antigens from coronavirus 229E and OC43. Infect. Immun. **35:**515–522.
32. **Simmons, G., J. D. Reeves, A. J. Rennekamp, S. M. Amberg, A. J. Piefer, and P. Bates.** 2004. Characterization of severe acute respiratory syndrome-associated coronavirus (SARS-CoV) spike glycoprotein-mediated viral entry. Proc. Natl. Acad. Sci. USA **101:**4240–4245.
33. **Simmons, G., D. N. Gosalia, A. J. Rennekamp, J. D. Reeves, S. L. Diamond, and P. Bates.** 2005. Inhibitors of cathepsin L prevent severe acute respiratory syndrome coronavirus entry. Proc. Natl. Acad. Sci. USA **102:**11876–11881.
34. **Snijder, E. J., P. J. Bredenbeek, J. C. Dobbe, V. Thiel, J. Ziebuhr, L. L. Poon, Y. Guan, M. Rozanov, W. J. Spaan, and A. E. Gorbalenya.** 2003. Unique and conserved features of genome and proteome of SARS-coronavirus, an early split-off from the coronavirus group 2 lineage. J. Mol. Biol. **331:**991–1004.
35. **Song, H. C., M. Y. Seo, K. Stadler, B. J. Yoo, Q. L. Choo, S. R. Coates, Y. Uematsu, T. Harada, C. E. Greer, J. M. Polo, P. Pileri, M. Eickmann, R. Rappuoli, S. Abrignani, M. Houghton, and J. H. Han.** 2004. Synthesis and characterization of a native, oligomeric form of recombinant severe acute respiratory syndrome coronavirus spike glycoprotein. J. Virol. **78:**10328–10335.
36. **Sturman, L. S., C. S. Richard, and K. V. Holmes.** 1985. Proteolytic cleavage of the E2 glycoprotein of murine coronavirus: activation of cell-fusing activ-

ity of virions by trypsin and separation of two different 90K cleavage fragment. J. Virol. **56**:904–911.
37. **Taguchi, F., and Y. K. Shimazaki.** 2000. Functional analysis of an epitope in the S2 subunit of the murine coronavirus spike protein: involvement in fusion activity. J. Gen. Virol. **81**:2867–2871.
38. **Ujike, M., H. Nishikawa, A. Otaka, N. Yamamoto, N. Yamamoto, M. Matsuoka, E. Kodama, N. Fujii, and F. Taguchi.** 2008. Heptad repeat-derived peptides block the protease-mediated direct entry from cell surface of SARS coronavirus but not entry via endosomal pathway. J. Virol. **82**:588–592.
39. **Weiss, S. R., and S. Navas-Martin.** 2005. Coronavirus pathogenesis and the emerging pathogen severe acute respiratory syndrome coronavirus. Microbiol. Mol. Biol. Rev. **69**:635–664.
40. **Xiao, X., S. Chakraborti, A. S. Dimitrov, K. Gramatikoff, and D. S. Dimitrov.** 2003. The SARS-CoV S glycoprotein: expression and functional characterization. Biochem. Biophys. Res. Commun. **312**:1159–1164.
41. **Yamada, Y. K., K. Takimoto, M. Yabe, and F. Taguchi.** 1997. Acquired fusion activity of a murine coronavirus MHV-2 variant with mutations in the proteolytic cleavage site and the signal sequence of the S protein. Virology **227**:215–219.

JOURNAL OF VIROLOGY, Jan. 2008, p. 588–592
0022-538X/08/$08.00+0 doi:10.1128/JVI.01697-07

Vol. 82, No. 1

Heptad Repeat-Derived Peptides Block Protease-Mediated Direct Entry from the Cell Surface of Severe Acute Respiratory Syndrome Coronavirus but Not Entry via the Endosomal Pathway▽

Makoto Ujike,[1]† Hiroki Nishikawa,[2]† Akira Otaka,[3] Naoki Yamamoto,[4] Norio Yamamoto,[4] Masao Matsuoka,[5] Eiichi Kodama,[5] Nobutaka Fujii,[2,5]* and Fumihiro Taguchi[1]*

Department of Virology III, National Institute of Infectious Disease, Gakuen 4-7-1, Musashi-murayama, Tokyo 208-0011, Japan[1]; Graduate School of Pharmaceutical Sciences, Kyoto University, Sakyo-ku, Kyoto 606-8501, Japan[2]; Graduate School of Pharmaceutical Sciences, The University of Tokushima, Tokushima 770-8505, Japan[3]; Department of Molecular Virology, Tokyo Medical and Dental University, 1-5-45 Yushima, Bunkyo-ku, Tokyo 113-8519, Japan[4]; and Institute for Virus Research, Kyoto University, Sakyo-ku, Kyoto 606-8507, Japan[5]

Received 6 August 2007/Accepted 6 October 2007

The peptides derived from the heptad repeat (HRP) of severe acute respiratory syndrome coronavirus (SCoV) spike protein (sHRPs) are known to inhibit SCoV infection, yet their efficacies are fairly low. Recently our research showed that some proteases facilitated SCoV's direct entry from the cell surface, resulting in a more efficient infection than the previously known infection via endosomal entry. To compare the inhibitory effect of the sHRP in each pathway, we selected two sHRPs, which showed a strong inhibitory effect on the interaction of two heptad repeats in a rapid and virus-free in vitro assay system. We found that they efficiently inhibited SCoV infection of the protease-mediated cell surface pathway but had little effect on the endosomal pathway. This finding suggests that sHRPs may effectively prevent infection in the lungs, where SCoV infection could be enhanced by proteases produced in this organ. This is the first observation that HRP exhibits different effects on virus that takes the endosomal pathway and virus that enters directly from the cell surface.

Severe acute respiratory syndrome (SARS) coronavirus (SCoV) is a causative agent of life-threatening SARS (4, 7, 15, 31). Although the first outbreak of SARS was stamped out, an effective antiviral drug is still required for the treatment and prevention of possible future outbreaks. SCoV is an enveloped virus and enters cells via fusion between the cellular membrane and its envelope. SCoV membrane fusion is mediated by the spike (S) protein, which is classified as a class I fusion protein. One of the most important features of class I fusion proteins is the conserved heptad repeat regions (HR1 and HR2) which play an essential role in virus-cell fusion activities (3, 6, 10, 28). In the fusion process, HR1 forms an interior, trimeric coiled-coil structure to which HR2 binds in an antiparallel fashion, resulting in the formation of a six-helix bundle. This structure brings viral and cellular membranes into close proximity to facilitate membrane fusion. Synthetic short peptides derived from the HR (HRP) of class I fusion proteins have been shown to block the interaction of HR1-HR2 complexes, resulting in the inhibition of a number of viral infections, including those of retroviruses (11, 14, 21, 23, 32, 38, 39), paramyxoviruses (12, 16, 30, 36, 42–44), filovirus (37), and coronavirus (2). Similarly, HRP of SCoV S (sHRP) could also inhibit SCoV and human immunodeficiency virus (HIV)/SCoV-pseudotyped virus infection (1, 18, 24, 45). However, these inhibitory effects were significantly less than those of one of the most effective HRPs from HIV type 1 (HIV-1) (39) and even those from the same family, murine coronavirus mouse hepatitis virus (MHV) (2).

The major organs targeted by SCoV are the lungs and intestines, although the virus grows in a variety of tissues that express angiotensin-converting enzyme 2 (ACE2). Recently we and others showed that SCoV uses two distinct entry pathways depending on the presence of proteases (20, 33, 34). In the absence of proteases, SCoV enters the cell via an endosomal pathway (9, 26, 41), with the S protein activated for fusion by the cathepsin L protease, which is active only under acidic conditions in the endosome (8, 33). In contrast, in the presence of protease, SCoV virion S proteins attach to ACE2 on the host cell surface and are activated for fusion by proteases such as trypsin or elastase, which leads to envelope-plasma membrane fusion and direct entry from the cell surface (20, 33, 34). Infection via the cell surface is more than 100 times more efficient than infection via the endosomal pathway (20). These results suggested the possibility that the severe illnesses in the lung and intestine could be due to the enhancement of direct SCoV cell surface entry mediated by proteases produced in these organs (20).

Although previous studies have described the inhibitory effects of the sHRP on SCoV infection via the endosomal path-

* Corresponding author. Mailing address for F. Taguchi: Department of Virology III, National Institute of Infectious Disease, Gakuen 4-7-1, Musashi-murayama, Tokyo 208-0011, Japan. Phone: 81-42-561-0771, ext. 533. Fax: 81-42-567-5631. E-mail: ftaguchi@nih.go.jp. Mailing address for N. Fujii: Graduate School of Pharmaceutical Sciences, Kyoto University, Sakyo-ku, Kyoto 606-8501, Japan. Phone: 81-75-753-4511. Fax: 81-75-753-4570. E-mail: nfujii@pharm.kyoto-u.ac.jp.
† M.U. and H.N. contributed equally to this work.
▽ Published ahead of print on 17 October 2007.

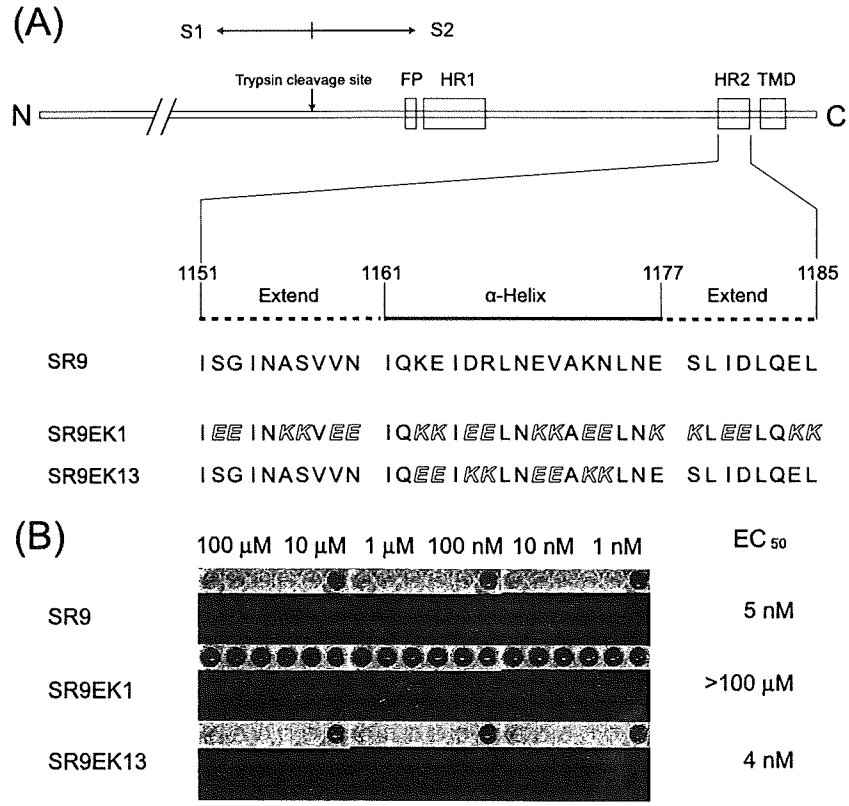

FIG. 1. (A) Schematic of SCoV S protein and sequences of native sHRP (SR9) and its EK substitution derivatives. The S protein contains two α-helical heptad repeats (HR1 and HR2), a putative fusion peptide (FP), a transmembrane domain (TMD), and a trypsin cleavage site (17). The expanded region shows the amino acid sequence of HR2 (SR9), which consists of two extended parts (1151 to 1160 and 1178 to 1185) and one α-helix part (1161 to 1177). Substituted EKs are shown with italic white letters. (B) In vitro binding inhibition assay of HRPs. GST-HR2-coated plates were incubated with MBP-HR1 in the presence of various concentrations (1 nM to 100 μM) of sHRP. Inhibitory potency of the peptide was assessed using the anti-MBP antibody-alkaline phosphatase conjugate and staining with 5-bromo-4-chloro-3-indolylphosphate.

way (1, 18, 24, 45), little is known about their effects on the protease-mediated cell surface pathway. Thus, in this study, we reevaluated the inhibitory effects of the sHRP on infection via the two distinct pathways of SCoV entry.

Recent studies of the X-ray crystal structure of the SCoV S HR1-HR2 complex have shown that the HR2 peptide consists of two extended regions and one α-helical region (35, 40). Since we have found that HRPs with replacement by the X-EE-XX-KK sequence in the HIV-1 HR2 region exhibited potent anti-HIV-1 activity (27), we chose to modify the α-helical region of HRP derived from SCoV S HR2 (sHRP) and also to prepare the control peptide SR9EK1 without sequence relatedness (Fig. 1A). To estimate these sHRPs, we established a rapid and virus-free in vitro novel assay system based on the inhibition of HR1-HR2 complex formation. Two fusion proteins (maltose binding protein [MBP]-HR1 [amino acid residues of the S protein, 892 to 964] and glutathione *S*-transferase [GST]-HR2 [1141 to 1192]) were expressed using *Escherichia coli* and purified using amylose resin (New England Biolabs) and glutathione Sepharose 4B (GE Healthcare, Bucks, United Kingdom), respectively. An enzyme-linked immunosorbent assay plate was coated with GST-HR2 dissolved in sodium carbonate buffer (pH 8.5), 3.6 μg/ml in concentration, by incubation at 4°C for 8 h. After bovine serum albumin blocking (1 mg/ml) at 4°C for 2.5 h, GST-HR2 on the plate was allowed to bind the MBP-HR1 protein (8.8 μg/ml) by incubation at 37°C for 1.5 h in the presence of various concentrations of sHRPs to be examined for inhibition activity. After the plate was washed, the inhibiting potency of the peptide was assessed by colorimetric analyses using the anti-MBP antibody-alkaline phosphatase conjugate (Sigma) with a 1:1,000 dilution with incubation at 4°C for 1 h and then staining with BluePhos microwell phosphatase (KPL). As shown in Fig. 1B, SR9 and SR9EK13 showed significant binding inhibition in a nanomolar range, whereas the control, SR9EK1, without sequence relatedness, had no inhibitory effect at a concentration of 100 μM.

We tested the inhibitory effects of SR9 and SR9EK13 on SCoV entry, since these sHRPs were found to have a strong binding inhibition activity, along with the control peptide SR9EK1. We examined their effects on both the endosomal and protease-mediated cell surface entry processes. Viral entry via the endosome was examined as described previously with a slight modification (20). In brief, VeroE6 cells were pretreated with each sHRP at 37°C for 30 min and then inoculated with SCoV (multiplicity of infection = 1.0) and incubated on ice for 30 min to allow viral attachment to ACE2 but not viral entry. After removal of unattached viruses, the cells were incubated at 37°C for 6 h. Viral entry was measured by quantifying the newly synthesized mRNA9 using real-time PCR (20). To evaluate entry via the cell surface, the cells were pretreated with 1

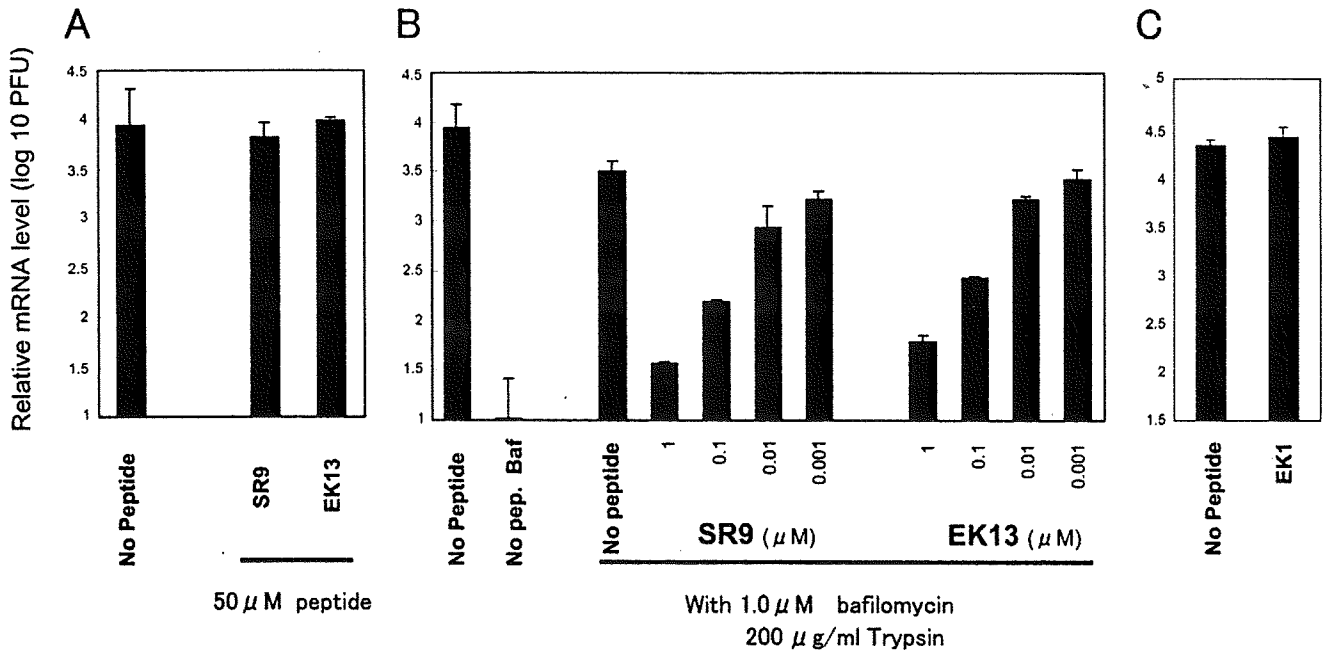

FIG. 2. Inhibitory effect of sHRPs on SCoV infections via the endosomal pathway (A) or protease-mediated cell-surface pathway (B). (A) VeroE6 cells were pretreated with 50 μM sHRPs at 37°C for 30 min, placed on ice for 10 min, and then inoculated with SCoV at a multiplicity of infection of 1.0 on ice for 30 min. After the removal of unbound virus, the cells were incubated in medium containing 50 μM sHRPs at 37°C for 6 h. (B) Cells pretreated with 1 μM Baf and sHRPs at the indicated concentrations were inoculated with SCoV as described above. After the removal of unbound virus, the cells were treated with 200 μg/ml L-1-tosylamide-2-phenylethyl chloromethyl ketone-treated trypsin at room temperature for 5 min and incubated at 37°C for 6 h. sHRP and Baf were present in the media in all steps at indicated concentrations. To measure amounts of viruses that entered cells, cells were infected with 10-fold-stepwise-diluted SARS-CoV from 10^6 to 10^2 PFU without Baf and trypsin and the amounts of mRNA9 were quantified by real-time PCR. Amounts of viral entry in this study were calculated from a calibration line obtained as described above and are shown as relative mRNA levels (20). (C) EK1 has no sequential similarity to sHRP and showed no inhibitory effect in vitro. Cells were treated with 1 μM EK1 as a control peptide, and other procedures were performed as described for panel B.

μM bafilomycin (Baf), which blocks SCoV endosomal entry, at 37°C for 30 min before SCoV inoculation. After removal of unattached viruses, the cells were treated with trypsin (0.2 mg/ml) for 5 min at room temperature and viral entry was measured as described above. Each sHRP and/or Baf was present in the media in all steps at various concentrations. In the absence of proteases, these sHRPs showed no measurable inhibitory effect on SCoV endosomal infection even at concentrations as high as 50 μM, despite showing a potent inhibitory effect in vitro (Fig. 2A). This lack of inhibition is consistent with previous observations that the same or homologous-sequence sHRPs had no inhibitory effect on SCoV infection at high concentrations of 10 μM (45) or 50 μM (1), respectively. In contrast, when SCoV was allowed to enter cells via the cell surface by treatment with protease and Baf, these sHRPs showed a strong inhibitory effect on SCoV infection in a dose-dependent manner (Fig. 2B). At a concentration of 0.1 μM, the SR9 sHRP reduced newly synthesized mRNA9 levels by about 10-fold, while an sHRP concentration of 1 μM saw a 50-fold decrease. The control sHRP, SR9EK1, did not inhibit SCoV cell-surface-mediated infection even at the concentration of 1 μM, indicating that the inhibition is peptide sequence specific (Fig. 2C). We finally evaluated the inhibitory effect of sHRPs in the presence of trypsin but without Baf treatment. These conditions may resemble the situation of patients with severe SARS, in which some proteases were produced in the infected lung and intestinal tissue. Under these conditions, these sHRPs also showed a potent inhibitory effect on SCoV infection (Fig. 3).

The present study indicates that our sHRPs fail to inhibit endosome-mediated SCoV infection. This finding is consistent with those of previous studies indicating that sHRPs have a low inhibitory effect on endosomal infection of native SCoV. The reported 50% effective dose (EC_{50}) was 3.68 to 19.0 μM (1, 18, 45). However, our results suggest that sHRPs, which showed no measurable inhibitory effect on SCoV endosomal infection, have a very strong inhibitory effect on protease-mediated cell surface SCoV infection; the EC_{50} was less than 100 nM (Fig. 2B and 3). Cell surface infection of SCoV is anticipated to occur in the lungs of SARS patients, since various types of inflammatory cells infiltrate the lung of the patients (25), and thus elastase, a protease produced in lung inflammation (13) and shown to enhance SCoV infection in cultured cells (20), could enhance SCoV infection in the lung by facilitating the infection from cell surface. Inhibitory effects of sHRPs on cell surface infection may help prevent severe damage by SCoV infection in the major target organ. Thus, the sHRPs shown in this study would be effective anti-SARS therapeutic drugs.

A few possibilities are conceivable for the explanation of an inefficient inhibitory effect of sHRPs in infection via the endosomal pathway. One is the failure of sHRPs to be trafficked to the endosome vehicles from culture medium. Thus, their concentration in the endosome is not sufficient to prevent SCoV infection. Alternatively, sHRPs may be sufficiently transported

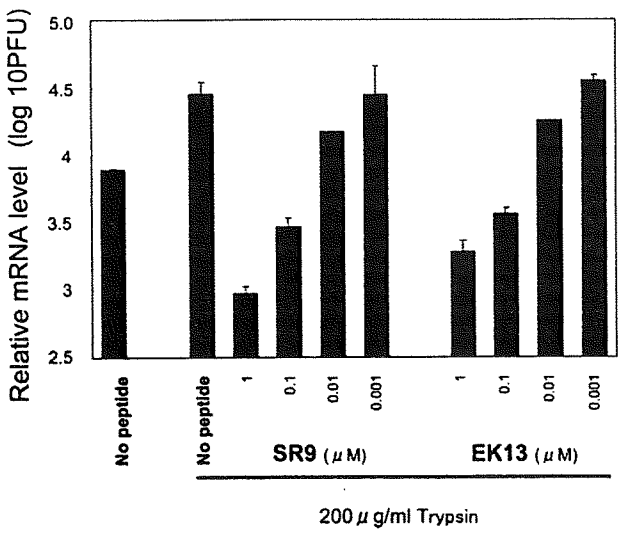

FIG. 3. Effective inhibition by HRPs of SCoV infection in the presence of exogenous trypsin. VeroE6 cells pretreated with sHRPs at the indicated concentrations were inoculated with SCoV as described in the legend to Fig. 2. After the removal of unbound virus, the cells were treated with 200 μg/ml L-1-tosylamide-2-phenylethyl chloromethyl ketone-treated trypsin at room temperature for 5 min and incubated at 37°C for 6 h. sHRPs were present in the media in all steps at the indicated concentrations. The relative viral mRNA9 was measured quantitatively by real-time PCR as described in the legend to Fig. 2. In this assay, cells were not treated with Baf throughout the experiment.

to the endosome but are inactivated by the low-pH environment or are degraded or digested with proteases present in the endosome. Another possibility is that the conformation of the cleaved S protein in the acidic environment of the endosome is different from that in a neutral pH and the sHRP fails to bind to the S protein in the former environment even if six-helix bundles with intramolecular HR2 are formed under both conditions. We are currently studying whether the inefficient inhibition of virus entry into cells could be attributed to one of those possibilities, or even another.

Interestingly, the EC_{50} (approximately 680 μM) of HRP of Ebola virus (37), which is thought to enter cells via an endosomal pathway, is remarkably higher than those of other viruses which enter cells directly from the cell surface. The inhibition with HRP of influenza virus infection, which also uses an endosomal pathway, has not yet been reported, even though its hemagglutinin protein is the prototype class I fusion protein and its cell entry mechanism has been extensively studied. In contrast, HRP of avian leucosis sarcoma virus, which uses the endosomal pathway, was reported to inhibit the infection fairly efficiently (EC_{50} = 25 to 170 nM) (5, 23). The inhibition, however, was executed during the conformational rearrangement of the envelope protein that occurs on the cell surface following attachment to the receptor and facilitates the exposure of HRs but not later than the transport into the endosome, where the avian leucosis sarcoma virus genome enters the cytoplasm by its envelope and endosomal membrane fusion in a low-pH environment (19, 22, 23). These observations together with those of the present study and others (1, 18, 24, 45) suggest that the HRPs have very low or little inhibitory effect in the endosome. If the above assumption is correct and the HRPs were designed to be efficiently transferred into the endosome and to be stable in the environment, they may be new antiviral candidates against those viruses that take the endosomal entry pathway, such as influenza virus, Ebola virus, and SCoV. Thus, detailed molecular studies on SCoV and the sHRP will provide a good model for the development and evaluation of such endosome-philic antiviral peptide inhibitors.

Recent studies have reported that the low inhibitory effect of the SCoV sHRP compared to that of the MHV HRP could be attributed to the weaker interaction of the SCoV S HR1-HR2 complex versus that of MHV S (1, 2). However, SCoV infection was efficiently blocked by sHRP under certain conditions, as revealed in this study; the concentration of sHRPs needed to inhibit SCoV infection is even lower than that required for MHV inhibition (1, 2). The apparent difference between MHV and SCoV infection is the pathway used to enter cells; the former enters directly from the cell surface, whereas the latter takes an endosomal pathway. Both MHV and SCoV infections were efficiently blocked when these viruses utilized the cell surface pathway for entry. These observations suggest that the lower HRP inhibitory effect on SCoV could be due to different entry pathways between SCoV and MHV rather than the weaker interaction of the HRP and SCoV S. To further explore this possibility, studies are ongoing to determine the effect of MHV sHRPs on infection by MHV-2, which, like SCoV, utilizes an endosomal infection pathway (29).

We thank Miyuki Kawase for her excellent technical assistance and Shutoku Matsuyama for his valuable discussions.

This work was financially supported by grants from the Ministry of Education, Culture, Sports, Science and Technology.

REFERENCES

1. **Bosch, B. J., B. E. Martina, R. Van Der Zee, J. Lepault, B. J. Haijema, C. Versluis, A. J. Heck, R. De Groot, A. D. Osterhaus, and P. J. Rottier.** 2004. Severe acute respiratory syndrome coronavirus (SARS-CoV) infection inhibition using spike protein heptad repeat-derived peptides. Proc. Natl. Acad. Sci. USA **101**:8455–8460.
2. **Bosch, B. J., R. van der Zee, C. A. de Haan, and P. J. Rottier.** 2003. The coronavirus spike protein is a class I virus fusion protein: structural and functional characterization of the fusion core complex. J. Virol. **77**:8801–8811.
3. **Chan, W. E., C. K. Chuang, S. H. Yeh, M. S. Chang, and S. S. Chen.** 2006. Functional characterization of heptad repeat 1 and 2 mutants of the spike protein of severe acute respiratory syndrome coronavirus. J. Virol. **80**:3225–3237.
4. **Drosten, C., S. Gunther, W. Preiser, S. van der Werf, H. R. Brodt, S. Becker, H. Rabenau, M. Panning, L. Kolesnikova, R. A. Fouchier, A. Berger, A. M. Burguiere, J. Cinatl, M. Eickmann, N. Escriou, K. Grywna, S. Kramme, J. C. Manuguerra, S. Muller, V. Rickerts, M. Sturmer, S. Vieth, H. D. Klenk, A. D. Osterhaus, H. Schmitz, and H. W. Doerr.** 2003. Identification of a novel coronavirus in patients with severe acute respiratory syndrome. N. Engl. J. Med. **348**:1967–1976.
5. **Earp, L. J., S. E. Delos, R. C. Netter, P. Bates, and J. M. White.** 2003. The avian retrovirus avian sarcoma/leukosis virus subtype A reaches the lipid mixing stage of fusion at neutral pH. J. Virol. **67**:3058–3066.
6. **Follis, K. E., J. York, and J. H. Nunberg.** 2005. Serine-scanning mutagenesis studies of the C-terminal heptad repeats in the SARS coronavirus S glycoprotein highlight the important role of the short helical region. Virology **341**:122–129.
7. **Fouchier, R. A., T. Kuiken, M. Schutten, G. van Amerongen, G. J. van Doornum, B. G. van den Hoogen, M. Peiris, W. Lim, K. Stohr, and A. D. Osterhaus.** 2003. Aetiology: Koch's postulates fulfilled for SARS virus. Nature **423**:240.
8. **Huang, I. C., B. J. Bosch, F. Li, W. Li, K. H. Lee, S. Ghiran, N. Vasilieva, T. S. Dermody, S. C. Harrison, P. R. Dormitzer, M. Farzan, P. J. Rottier, and H. Choe.** 2006. SARS coronavirus, but not human coronavirus NL63, utilizes cathepsin L to infect ACE2-expressing cells. J. Biol. Chem. **281**:3198–3203.
9. **Inoue, Y., N. Tanaka, Y. Tanaka, S. Inoue, K. Morita, M. Zhuang, T. Hattori, and K. Sugamura.** 2007. Clathrin-dependent entry of severe acute respira-

tory syndrome coronavirus into target cells expressing ACE2 with the cytoplasmic tail deleted. J. Virol. **81:**8722–8729.
10. **Jahn, R., T. Lang, and T. C. Sudhof.** 2003. Membrane fusion. Cell **112:**519–533.
11. **Jiang, S., K. Lin, N. Strick, and A. R. Neurath.** 1993. HIV-1 inhibition by a peptide. Nature **365:**113.
12. **Joshi, S. B., R. E. Dutch, and R. A. Lamb.** 1998. A core trimer of the paramyxovirus fusion protein: parallels to influenza virus hemagglutinin and HIV-1 gp41. Virology **248:**20–34.
13. **Kawabata, K., T. Hagio, and S. Matsuoka.** 2002. The role of neutrophil elastase in acute lung injury. Eur. J. Pharmacol. **451:**1–10.
14. **Kilby, J. M., S. Hopkins, T. M. Venetta, B. DiMassimo, G. A. Cloud, J. Y. Lee, L. Alldredge, E. Hunter, D. Lambert, D. Bolognesi, T. Matthews, M. R. Johnson, M. A. Nowak, G. M. Shaw, and M. S. Saag.** 1998. Potent suppression of HIV-1 replication in humans by T-20, a peptide inhibitor of gp41-mediated virus entry. Nat. Med. **4:**1302–1307.
15. **Ksiazek, T. G., D. Erdman, C. S. Goldsmith, S. R. Zaki, T. Peret, S. Emery, S. Tong, C. Urbani, J. A. Comer, W. Lim, P. E. Rollin, S. F. Dowell, A. E. Ling, C. D. Humphrey, W. J. Shieh, J. Guarner, C. D. Paddock, P. Rota, B. Fields, J. DeRisi, J. Y. Yang, N. Cox, J. M. Hughes, J. W. LeDuc, W. J. Bellini, and L. J. Anderson.** 2003. A novel coronavirus associated with severe acute respiratory syndrome. N. Engl. J. Med. **348:**1953–1966.
16. **Lambert, D. M., S. Barney, A. L. Lambert, K. Guthrie, R. Medinas, D. E. Davis, T. Bucy, J. Erickson, G. Merutka, and S. R. Petteway, Jr.** 1996. Peptides from conserved regions of paramyxovirus fusion (F) proteins are potent inhibitors of viral fusion. Proc. Natl. Acad. Sci. USA **93:**2186–2191.
17. **Li, F., M. Berardi, W. Li, M. Farzan, P. R. Dormitzer, and S. C. Harrison.** 2006. Conformational states of the severe acute respiratory syndrome coronavirus spike protein ectodomain. J. Virol. **80:**6794–6800.
18. **Liu, S., G. Xiao, Y. Chen, Y. He, J. Niu, C. R. Escalante, H. Xiong, J. Farmar, A. K. Debnath, P. Tien, and S. Jiang.** 2004. Interaction between heptad repeat 1 and 2 regions in spike protein of SARS-associated coronavirus: implications for virus fusogenic mechanism and identification of fusion inhibitors. Lancet **363:**938–947.
19. **Matsuyama, S., S. E. Delos, and J. M. White.** 2004. Sequential roles of receptor binding and low pH in forming prehairpin and hairpin conformations of a retroviral envelope glycoprotein. J. Virol. **78:**8201–8209.
20. **Matsuyama, S., M. Ujike, S. Morikawa, M. Tashiro, and F. Taguchi.** 2005. Protease-mediated enhancement of severe acute respiratory syndrome coronavirus infection. Proc. Natl. Acad. Sci. USA **102:**12543–12547.
21. **Medinas, R. J., D. M. Lambert, and W. A. Tompkins.** 2002. C-Terminal gp40 peptide analogs inhibit feline immunodeficiency virus: cell fusion and virus spread. J. Virol. **76:**9079–9086.
22. **Melikyan, G. B., R. J. Barnard, R. M. Markosyan, J. A. Young, and F. S. Cohen.** 2004. Low pH is required for avian sarcoma and leukosis virus Env-induced hemifusion and fusion pore formation but not for pore growth. J. Virol. **78:**3753–3762.
23. **Netter, R. C., S. M. Amberg, J. W. Balliet, M. J. Biscone, A. Vermeulen, L. J. Earp, J. M. White, and P. Bates.** 2004. Heptad repeat 2-based peptides inhibit avian sarcoma and leukosis virus subgroup a infection and identify a fusion intermediate. J. Virol. **78:**13430–13439.
24. **Ni, L., J. Zhu, J. Zhang, M. Yan, G. F. Gao, and P. Tien.** 2005. Design of recombinant protein-based SARS-CoV entry inhibitors targeting the heptad-repeat regions of the spike protein S2 domain. Biochem. Biophys. Res. Commun. **330:**39–45.
25. **Nicholls, J. M., L. L. Poon, K. C. Lee, W. F. Ng, S. T. Lai, C. Y. Leung, C. M. Chu, P. K. Hui, K. L. Mak, W. Lim, K. W. Yan, K. H. Chan, N. C. Tsang, Y. Guan, K. Y. Yuen, and J. S. Peiris.** 2003. Lung pathology of fatal severe acute respiratory syndrome. Lancet **361:**1773–1778.
26. **Nie, Y., P. Wang, X. Shi, G. Wang, J. Chen, A. Zheng, W. Wang, Z. Wang, X. Qu, M. Luo, L. Tan, X. Song, X. Yin, J. Chen, M. Ding, and H. Deng.** 2004. Highly infectious SARS-CoV pseudotyped virus reveals the cell tropism and its correlation with receptor expression. Biochem. Biophys. Res. Commun. **321:**994–1000.
27. **Otaka, A., M. Nakamura, D. Nameki, E. Kodama, S. Uchiyama, S. Nakamura, H. Nakano, H. Tamamura, Y. Kobayashi, M. Matsuoka, and N. Fujii.** 2002. Remodeling of gp41-C34 peptide leads to highly effective inhibitors of the fusion of HIV-1 with target cells. Angew. Chem. Int. Ed. Engl. **41:**2937–2940.
28. **Petit, C. M., J. M. Melancon, V. N. Chouljenko, R. Colgrove, M. Farzan, D. M. Knipe, and K. G. Kousoulas.** 2005. Genetic analysis of the SARS-coronavirus spike glycoprotein functional domains involved in cell-surface expression and cell-to-cell fusion. Virology **341:**215–230.
29. **Qiu, Z., S. T. Hingley, G. Simmons, C. Yu, J. Das Sarma, P. Bates, and S. R. Weiss.** 2006. Endosomal proteolysis by cathepsins is necessary for murine coronavirus mouse hepatitis virus type 2 spike-mediated entry. J. Virol. **80:**5768–5776.
30. **Rapaport, D., M. Ovadia, and Y. Shai.** 1995. A synthetic peptide corresponding to a conserved heptad repeat domain is a potent inhibitor of Sendai virus-cell fusion: an emerging similarity with functional domains of other viruses. EMBO J. **14:**5524–5531.
31. **Rota, P. A., M. S. Oberste, S. S. Monroe, W. A. Nix, R. Campagnoli, J. P. Icenogle, S. Penaranda, B. Bankamp, K. Maher, M. H. Chen, S. Tong, A. Tamin, L. Lowe, M. Frace, J. L. DeRisi, Q. Chen, D. Wang, D. D. Erdman, T. C. Peret, C. Burns, T. G. Ksiazek, P. E. Rollin, A. Sanchez, S. Liffick, B. Holloway, J. Limor, K. McCaustland, M. Olsen-Rasmussen, R. Fouchier, S. Gunther, A. D. Osterhaus, C. Drosten, M. A. Pallansch, L. J. Anderson, and W. J. Bellini.** 2003. Characterization of a novel coronavirus associated with severe acute respiratory syndrome. Science **300:**1394–1399.
32. **Sagara, Y., Y. Inoue, H. Shiraki, A. Jinno, H. Hoshino, and Y. Maeda.** 1996. Identification and mapping of functional domains on human T-cell lymphotropic virus type 1 envelope proteins by using synthetic peptides. J. Virol. **70:**1564–1569.
33. **Simmons, G., D. N. Gosalia, A. J. Rennekamp, J. D. Reeves, S. L. Diamond, and P. Bates.** 2005. Inhibitors of cathepsin L prevent severe acute respiratory syndrome coronavirus entry. Proc. Natl. Acad. Sci. USA **102:**11876–11881.
34. **Simmons, G., J. D. Reeves, A. J. Rennekamp, S. M. Amberg, A. J. Piefer, and P. Bates.** 2004. Characterization of severe acute respiratory syndrome-associated coronavirus (SARS-CoV) spike glycoprotein-mediated viral entry. Proc. Natl. Acad. Sci. USA **101:**4240–4245.
35. **Supekar, V. M., C. Bruckmann, P. Ingallinella, E. Bianchi, A. Pessi, and A. Carfi.** 2004. Structure of a proteolytically resistant core from the severe acute respiratory syndrome coronavirus S2 fusion protein. Proc. Natl. Acad. Sci. USA **101:**17958–17963.
36. **Wang, E., X. Sun, Y. Qian, L. Zhao, P. Tien, and G. F. Gao.** 2003. Both heptad repeats of human respiratory syncytial virus fusion protein are potent inhibitors of viral fusion. Biochem. Biophys. Res. Commun. **302:**469–475.
37. **Watanabe, S., A. Takada, T. Watanabe, H. Ito, H. Kida, and Y. Kawaoka.** 2000. Functional importance of the coiled-coil of the Ebola virus glycoprotein. J. Virol. **74:**10194–10201.
38. **Wild, C., T. Oas, C. McDanal, D. Bolognesi, and T. Matthews.** 1992. A synthetic peptide inhibitor of human immunodeficiency virus replication: correlation between solution structure and viral inhibition. Proc. Natl. Acad. Sci. USA **89:**10537–10541.
39. **Wild, C. T., D. C. Shugars, T. K. Greenwell, C. B. McDanal, and T. J. Matthews.** 1994. Peptides corresponding to a predictive alpha-helical domain of human immunodeficiency virus type 1 gp41 are potent inhibitors of virus infection. Proc. Natl. Acad. Sci. USA **91:**9770–9774.
40. **Xu, Y., Z. Lou, Y. Liu, H. Pang, P. Tien, G. F. Gao, and Z. Rao.** 2004. Crystal structure of severe acute respiratory syndrome coronavirus spike protein fusion core. J. Biol. Chem. **279:**49414–49419.
41. **Yang, Z. Y., Y. Huang, L. Ganesh, K. Leung, W. P. Kong, O. Schwartz, K. Subbarao, and G. J. Nabel.** 2004. pH-dependent entry of severe acute respiratory syndrome coronavirus is mediated by the spike glycoprotein and enhanced by dendritic cell transfer through DC-SIGN. J. Virol. **78:**5642–5650.
42. **Yao, Q., and R. W. Compans.** 1996. Peptides corresponding to the heptad repeat sequence of human parainfluenza virus fusion protein are potent inhibitors of virus infection. Virology **223:**103–112.
43. **Young, J. K., D. Li, M. C. Abramowitz, and T. G. Morrison.** 1999. Interaction of peptides with sequences from the Newcastle disease virus fusion protein heptad repeat regions. J. Virol. **73:**5945–5956.
44. **Yu, M., E. Wang, Y. Liu, D. Cao, N. Jin, C. W. Zhang, M. Bartlam, Z. Rao, P. Tien, and G. F. Gao.** 2002. Six-helix bundle assembly and characterization of heptad repeat regions from the F protein of Newcastle disease virus. J. Gen. Virol. **83:**623–629.
45. **Yuan, K., L. Yi, J. Chen, X. Qu, T. Qing, X. Rao, P. Jiang, J. Hu, Z. Xiong, Y. Nie, X. Shi, W. Wang, C. Ling, X. Yin, K. Fan, L. Lai, M. Ding, and H. Deng.** 2004. Suppression of SARS-CoV entry by peptides corresponding to heptad regions on spike glycoprotein. Biochem. Biophys. Res. Commun. **319:**746–752.

Clinical and Immunological Response to Attenuated Tissue-Cultured Smallpox Vaccine LC16m8

Tomoya Saito, MD, PhD
Tatsuya Fujii, MD
Yasuhiro Kanatani, MD, PhD
Masayuki Saijo, MD, PhD
Shigeru Morikawa, DVM, PhD
Hiroyuki Yokote, MS
Tsutomu Takeuchi, MD, PhD
Noriyuki Kuwabara, MD, PhD

Context The attenuated, tissue-cultured, third-generation smallpox vaccine LC16m8 was administered to vaccinia-naive infants in Japan during the 1970s without serious adverse events. It is a good candidate for use as part of a prevention plan for bioterrorism.

Objective To assess the immunogenicity and frequency of adverse events of LC16m8 vaccine in unvaccinated and previously vaccinated adults.

Design, Setting, and Participants Between 2002 and 2005 we vaccinated and revaccinated 1529 and 1692 adults, respectively, in the Japan Self-Defense Forces with LC16m8 vaccine, given intraepidermally using a bifurcated needle. Vaccinees were examined 10 to 14 days after vaccination to determine if they had developed a major skin reaction ("take"). Neutralizing antibody responses among 200 participants were assessed using a plaque-reduction neutralization test 30 days postvaccination. We monitored vaccinees for adverse events for 30 days postvaccination.

Main Outcome Measures Documentation of a vaccine take, presence of neutralizing antibody response, and frequency of adverse events.

Results The proportions of take in vaccinia-naive and previously vaccinated individuals were 1443 of 1529 (94.4% [95% confidence interval {CI}, 93.2%-95.9%] and 1465 of 1692 (86.6% [95% CI, 85.0%-88.2%]), respectively. Seroconversion or an effective booster response among the individuals with take was elicited in 37 of 41 (90.2% [95% CI, 81.2%-99.3%]) vaccinia-naive participants and in 93 of 155 (60.0% [95% CI, 52.3%-67.7%]) previously vaccinated participants. One case of allergic dermatitis and another of erythema multiforme, both of which were mild and self-limited, were suspected to be caused by vaccination. No severe adverse events were observed.

Conclusion Administration of an attenuated tissue-cultured smallpox vaccine (LC16m8) to healthy adults was associated with high levels of vaccine take and seroconversion in those who were vaccinia-naive and yielded an effective booster response in some previously vaccinated individuals.

JAMA. 2009;301(10):1025-1033 www.jama.com

THE THREAT OF SMALLPOX BIOterrorism has prompted reconsideration of the need for smallpox vaccination.[1-3] Serious adverse events associated with first-generation vaccines such as the New York City Board of Health (Dryvax; Wyeth, Madison, New Jersey), Lister, and Ikeda strains[4-8] have raised obstacles to vaccination campaigns in the United States.[7-9] Second-generation vaccines such as ACAM2000 (Acambis, Cambridge, Massachusetts) that use a first-generation seed virus but are grown in tissue culture are also usually accompanied by a high frequency of adverse events.[10] Developing a vaccine that is safer than first-generation vaccines yet highly immunogenic is crucial to constructing a prevention plan in the event of bioterrorist attack.

LC16m8 is a live, attenuated, tissue-cultured third-generation vaccine comprising attenuated vaccinia virus strains as well as subunit vaccines made from viral proteins or DNA.[11] It is a desirable candidate for routine vaccination because of its low reactogenicity and reasonable safety profile.[12] Vaccination can be conveniently accomplished with a single intraepidermal scarification alone, which usually results in a visible major skin reaction ("take") similar to those resulting from first- and second-generation vaccines.[13]

LC16m8 was derived from the Lister strain used for the Intensified Smallpox Eradication Programme of the World Health Organization[4] by temperature sensitivity and pock size

See also Patient Page.

Author Affiliations: Bio-preparedness Research Laboratory, Department of Tropical Medicine and Parasitology, School of Medicine, Keio University, Tokyo, Japan (Drs Saito and Takeuchi); Department of Internal Medicine (Dr Fujii) and Center for Health Management (Dr Kuwabara), Japan Self-Defense Forces Central Hospital, Tokyo; Research Institute, National Defense Medical College, Saitama, Japan (Dr Kanatani); Department of Virology I, National Institute of Infectious Diseases, Tokyo (Drs Saijo and Morikawa); and Chemo-Sero-Therapeutic Research Institute (Kaketsuken), Kumamoto, Japan (Mr Yokote).
Corresponding Author: Yasuhiro Kanatani, MD, PhD, National Defense Medical College, 3-2 Namiki, Tokorozawa-city, Saitama 359-8513, Japan (ykanatan@ndmc.ac.jp).

Table 1. Age Group and Previous Vaccination History

		Vaccine Strains Used in Previous Vaccination		
Group	Birth Year	First Dose	Second Dose	Third Dose
A	1976-1984	Not vaccinated	Not vaccinated	Not vaccinated
B	1970-1975	Lister	Not vaccinated	Not vaccinated
C	1964-1969	Ikeda	Lister	Not vaccinated
D	1953-1963	Ikeda	Ikeda	Ikeda or Lister

through plaque cloning in rabbit kidney cells.[12] Clones were selected as vaccine candidates based on their high immunogenicity and safety properties in animal studies.[13] After a clinical trial enrolling approximately 10 000 children, Japanese health authorities administered LC16m8 vaccine to more than 100 000 infants between 1973 and the beginning of 1976, without serious adverse events.[14] Evaluation of the proportion of takes and presence of neutralizing antibody titer in vaccinia-naive children given LC16m8 vaccine showed a level of immunogenicity comparable with that achieved with the original Lister vaccine.[14] The LC16m8 vaccine has not been tested against smallpox (ie, variola virus) in the field, but challenge studies using pathogenic orthopoxviruses in animals have been successful.[15-18]

We examined the clinical and immunological responses to LC16m8 vaccine in vaccinia-naive and previously vaccinated adults to assess immunogenicity and safety. We measured clinical take, neutralizing antibody response, and frequency of adverse events as part of an adult vaccination program in the Japanese Self-Defense Forces.

METHODS

Vaccine

We vaccinated participants with licensed LC16m8 vaccine (lot No. Chiba 02; Kaketsuken, Kumamoto, Japan) containing a suspension of greater than 1×10^8 pock-forming units (pfu)/mL of the LC16m8 strain.

Study Design and Participants

The Self-Defense Forces Central Hospital planned and organized the smallpox vaccination program for select personnel in the Japan Self-Defense Forces. Candidates were participants in the International Peacekeeping Operation activities of the United Nations Disengagement Observer Force.[19] Study participants were enrolled in a vaccination program adhering to a guideline,[20] completing 6 rounds of vaccination from 2002 to 2005. Approximately 350 to 700 healthy adults aged 18 to 55 years were recruited in each round. Individuals providing written informed consent were screened for contraindications using a questionnaire as well as an interview with a physician before vaccination.

Inclusion criteria for vaccination were (1) normal renal and hepatic function as indicated by urine dipstick testing and measurement of serum levels of aspartate aminotransferase, alanine aminotransferase, and alkaline transferase; (2) negative test results for hepatitis B surface antigen, hepatitis C antibodies, and human T-cell lymphotropic virus; (3) no history of human immunodeficiency virus infection; and (4) normal hematology parameters (white blood cell count, red blood cell count, platelet count).

Exclusion criteria were (1) pregnancy; (2) underlying immunosuppression or treatment with immunosuppressive drugs; (3) current eczema or other skin problems; (4) household contact with a person having any of the above; (5) receipt of another live attenuated-virus vaccine within 30 days; and (6) occupational exposure to pregnant women and newborn infants. Individuals with atopic dermatitis were vaccinated if skin lesions were dry and stable.

Participants were inoculated with approximately 4 μL of vaccine suspension (1×10^8 pfu/mL) using a disposable bifurcated needle (JMS Co Ltd, Hiroshima, Japan). Vaccinia-naive individuals (primary vaccinees) received 5 strokes, whereas previously vaccinated individuals (revaccinees) received 10 strokes. We defined vaccination history by visual examination of the scar before vaccination by the physician. Distinction between previous smallpox vaccination and bacille Calmette-Guérin can be made in Japan, because subcutaneous multiple puncture has been used for bacille Calmette-Guérin inoculation and results in a distinctively different scar.

For comparison, vaccinees were divided into 4 age groups (A-D) that most reasonably captured birth cohorts with different histories of previous vaccination (TABLE 1). In Japan, universal smallpox vaccination programs included 3 doses (birth, age 6 years, and age 12 years).[21] Because of the cessation of routine vaccination in early 1976, participants born after this (group A) were considered primary vaccinees. Based on the routine vaccination schedule before 1976, the birth cohort born from 1970 through 1975 (group B) was vaccinated once with the Lister strain. Birth cohorts from 1964 through 1969 (group C) were vaccinated with the Ikeda strain for the first dose and the Lister strain for the second. Participants born before 1964 (group D) were vaccinated with the Ikeda strain for the first and second doses and with either the Ikeda or Lister strain for the third.

We monitored participants for 30 days postvaccination. Successful vaccination was determined by the appearance of a major skin reaction (vaccine take), defined as a "pustular lesion or an area of definite induration or congestion surrounding a central lesion, which could be a scab or an ulcer,"[22] 10 to 14 days postvaccination.[20] To precisely assess the size of skin reaction yet avoid excessive reporting burden in a single vaccination round, the diameter of the local skin reaction on day 14 was measured among third-round vaccinees.

Serum samples were collected before and 30 days after vaccination from individuals vaccinated in the second round and were stored at −80°C until testing for neutralizing antibody titers and levels of troponin T.

The protocol was approved by the institutional review board of the Self-Defense Forces Central Hospital (No. 16-004; August 30, 2004).

Analysis of Serum Antibody Response

Neutralizing antibody levels to LC16m8 were assessed by plaque-reduction neutralization testing of serum specimens collected before and 30 days after vaccination. Effective seroconversion or booster response was defined as a 4-fold increase in plaque-reduction neutralization titer at day 30 after vaccination, compared with the titer before vaccination.

We determined the plaque-reduction neutralizing titer to LC16m8 (PRN_{LC16m8} titer) as follows. Heat-inactivated serum samples (20 minutes at 60°C) were serially diluted 4-fold, mixed with an equal volume of vaccinia LC16m8 virus that had been freshly sonicated, and then diluted to contain approximately 30 to 50 pfu/mL of virus.[23] Serum-virus mixtures were incubated overnight (approximately 15-18 hours) at 35°C with 5% CO_2, inoculated onto duplicate RK13 cell monolayers, and incubated 2 additional hours under identical conditions. After adsorption, RK-13 monolayers were overlaid with minimum essential medium supplemented with 5% fetal bovine serum and 0.8% agarose and then returned to the 35°C incubator for 3 days. At the end of the incubation period, monolayers were stained with neutral red, further incubated overnight at 35°C with 5% CO_2, and the plaques counted.

We defined the end point titer as the reciprocal of the highest dilution of serum with a mean plaque count of 50% or less plaque reduction. The 50% neutralization titer for each sample was calculated using Minitab Probit statistical analysis (Minitab Inc, State College, Pennsylvania) and converted to the dose required to produce infection in 50% of participants based on the concentration of undiluted product. Titers less than 1:4 were expressed as 2 and those less than 1:8 as 4 in the LC16m8 assay.

Frequency of Adverse Events

Vaccinees were interviewed for general health at the examination for take 10 to 14 days postvaccination. Vaccinees underwent electrocardiography (ECG) 30 days postvaccination. Those reporting symptoms suggestive of severe adverse events within 30 days postvaccination and those who exhibited a serious abnormality on ECG were hospitalized, monitored, and their severe adverse events reported. The incidence of minor adverse events was reviewed retrospectively using postvaccination records from individuals vaccinated during the third and fourth rounds. Serum samples obtained before and 30 days after vaccination were assayed for levels of troponin T, using electrochemiluminescence immunoassay (BML Inc, Tokyo, Japan), to screen for asymptomatic myopericarditis.

Statistical Analysis

We measured (1) vaccine take, (2) PRN_{LC16m8} titer, (3) seroconversion or effective boosting, (4) incidence of a specific adverse event, and (5) postvaccination day of adverse events. Outcomes 1, 3, and 4 were measured as dichotomous variables, whereas outcomes 2 and 5 were modeled as continuous variables. Outcomes 1, 2, and 3 were compared by age group (ordinal variable) and vaccination history (dichotomous). Dichotomous outcome variables and explanatory variables were compared using the χ^2 test. Neutralizing antibody titers were compared following logarithmic transformation, because the distribution of titers tended to skew toward the right.

We compared the PRN_{LC16m8} (or PRN_{Dryvax}) titers from different age groups using an independent-sample *t* test following the F test. We used the Mann-Whitney test for comparison between 2 groups because the postvaccination day of an adverse event is a discrete variable. $P = .05$ was considered significant; all statistical tests were 2-tailed. All analyses were performed using STATA version 9.2 (StataCorp, College Station, Texas).

Sample Size for Adverse Events

A total of 3221 vaccinees were monitored for severe adverse events; 1239 individuals vaccinated in the third and fourth rounds were more closely monitored for minor adverse events. To ensure the absence of a severe adverse event, believed to occur with a frequency of 2 per 100 000 individuals,[24] the study would require monitoring of 124 600 vaccinated individuals for a 95% level of significance. Our study yielded a significance level of 12.6% and an upper confidence limit of 2.5 cases. If the expected frequency were much greater (eg, 1 in 5000), the level of significance to ensure the absence of a severe adverse event in the present study would be increased to 72.4%.

The expected frequency of a common minor adverse event (eg, fever) is 4% to 6%,[2] and provided that vaccination with LC16m8 can reduce this frequency by 40% to 60% (ie, reduction of relative risk), the detection of a minor event with statistical power of 80% to 90% suggests that the minimum number of samples would be between 184 and 1021 individuals. This was met by our cohort of patients vaccinated in the third and fourth rounds (n = 1239). We assessed the representativeness of third- and fourth-round vaccinees compared with those in the other rounds by comparison of demographics (age, sex, vaccination history) and outcome (ie, take).

RESULTS

Vaccine Take

We enrolled 3468 persons in the program from 2002 to 2005, of whom 229 and 18 were not vaccinated owing to nonmedical or medical reasons, respectively (FIGURE 1). Those who did not receive vaccination owing to

Figure 1. Flow of Participants Through the Study

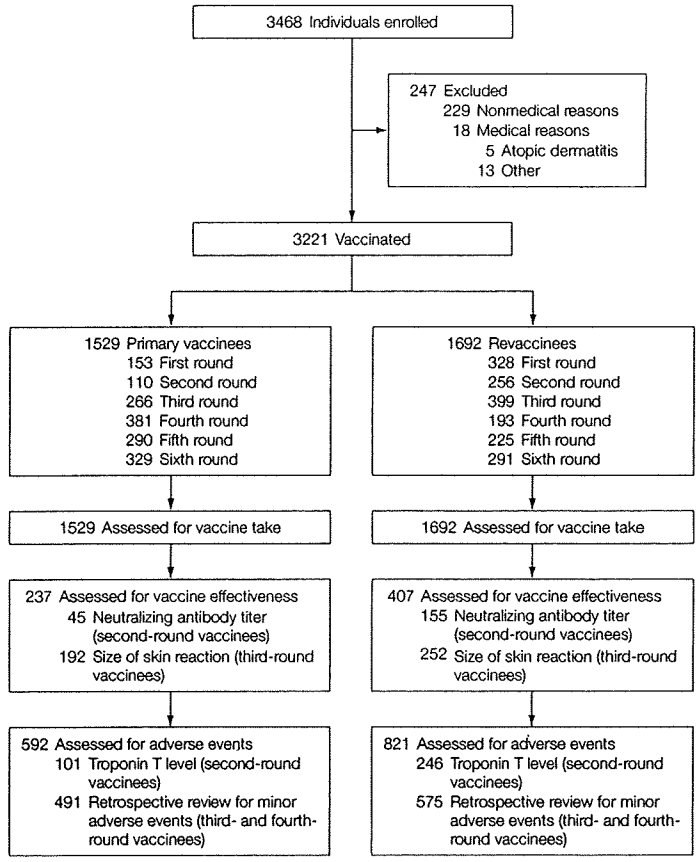

Candidates for the study were participants in the International Peacekeeping Operation activities of the United Nations Disengagement Observer Force enrolled in the vaccination program between 2002 and 2005.

nonmedical reasons accounted for only 6.6% of the total number of participants. Among those who did not receive vaccination owing to medical reasons, 5 had active atopic dermatitis. Four other individuals with a history of atopic dermatitis did receive vaccination because their skin lesions were not active.

In total, 3221 individuals (92.8% of all candidates) were vaccinated, and all underwent follow-up for 10 to 14 days to determine take. Nearly half (1529/3221 [47.5%]) had never been vaccinated, almost all were men (3168/3221 [98.4%]), and all were Asian.

The overall proportion of clinical take was significantly higher in primary vaccinees (1443/1529 [94.4%; 95% confidence interval {CI}, 93.2%-95.9%]) than in revaccinees (1465/1692 [86.6%; 95% CI, 85.0%-88.2%]) ($P<.001$) (TABLE 2). The proportion of takes induced by LC16m8 vaccine in primary vaccinees appeared comparable with the proportion induced by past vaccination with Lister strains and appeared slightly smaller than that induced by Dryvax. The proportion of takes did not significantly differ among age groups in primary vaccinees (Table 2). Among revaccinees, the 20- to 29-year-old age

Table 2. Proportion of Vaccine Take by Age and Vaccination Round in the Smallpox Vaccination Program With LC16m8

Round	No./Total by Age, y						% Take (95% CI)	*P* Value[a]
	<20	20-29	30-39	40-49	>50	Total		
Primary Vaccinees								
First	0/0	106/113	29/38	0/1	1/1	136/153	88.9 (83.9-93.9)	
Second	1/1	105/109	0/0	0/0	0/0	106/110	96.4 (92.9-99.9)	
Third	2/2	223/238	24/25	1/1	0/0	250/266	94.0 (91.1-96.8)	
Fourth	3/3	204/222	146/156	0/0	0/0	353/381	92.7 (90.0-95.3)	.003
Fifth	1/1	187/196	74/76	16/16	1/1	279/290	96.2 (94.0-98.4)	
Sixth	0/0	236/244	70/72	12/12	1/1	319/329	97.0 (95.1-98.8)	
Total	**7/7**	**1061/1122**	**343/367**	**29/30**	**3/3**	**1443/1529**	**94.4 (93.2-95.9)**	
% Take (95% CI)	100	94.6 (93.2-95.6)	93.5 (90.9-96.0)	96.7 (90.2-100)	100 (NA)			.82
Revaccinees								
First	0/0	1/1	106/161	93/147	12/19	212/328	64.6 (59.5-69.8)	
Second	0/0	54/54	136/136	61/61	5/5	256/256	100 (NA)	
Third	0/0	11/14	158/200	138/169	12/16	319/399	79.9 (76.0-83.9)	
Fourth	0/0	10/10	40/43	114/120	19/20	183/193	94.8 (91.7-97.9)	<.001
Fifth	0/0	4/5	137/145	60/67	8/8	209/225	92.9 (89.5-96.2)	
Sixth	0/0	0/0	187/191	95/96	4/4	286/291	98.3 (96.8-99.8)	
Total	**0/0**	**80/84**	**764/876**	**561/660**	**60/72**	**1465/1692**	**86.6 (85.0-88.2)**	
% Take (95% CI)		95.2 (90.7-99.8)	87.2 (85.0-89.4)	85.0 (82.3-87.7)	83.3 (74.7-91.9)			.05

Abbreviations: CI, confidence interval; NA, not available (not calculable).
[a] By χ^2 test.

group experienced a marginally higher proportion of takes compared with older age groups.

Size of Skin Reaction

We examined the local skin reaction and measured the diameter of the erythematous area in 665 third-round vaccinees. Among 569 participants with take, 444 (78.0%) local skin reactions were reported. The mean diameter of the erythematous area on day 14 was 12.0 (SD, 7.1) mm (n=192) in primary vaccinees and 7.5 (SD, 5.2 mm) (n=252) in revaccinees (FIGURE 2), both of which were considerably smaller than the 15.9 mm reported in infants on day 14 after vaccination.[14]

Level of Neutralizing Antibodies in Serum

Antibody testing performed on 200 serum samples from a total of 366 (54.6%) available from second-round vaccinees included 45, 47, 45, and 63 samples from age groups A, B, C, and D, respectively. The age at which revaccinees were sampled, stratified by previous vaccination history, was significantly older compared with nonsampled vaccinees ($P=.40$ and $P<.001$ for previously unvaccinated and vaccinated, respectively). We therefore stratified the analyses by age group whenever we analyzed the results of serum samples. Four of 45 individuals (8.9%) in age group A did not show clinical take and were therefore omitted from the analyses. Of the 4 individuals without take, 1 revealed seroconversion with PRN_{LC16m8}, although all did not seroconvert with PRN_{Dryvax}.

We compared PRN_{LC16m8} titer as well as the percentage of participants who seroconverted or experienced an effective booster response among the primary vaccinees and revaccinees as well as within revaccinees in different age groups (TABLE 3). Before vaccination, the geometric mean PRN_{LC16m8} titer in revaccinees (age groups B-D) was significantly higher than that in primary vaccinees (group A) ($P<.001$); the titer among participants in group D was higher than that in any other age group (B vs D, $P=.003$; C vs D, $P=.04$). After vaccination, the geometric mean PRN_{LC16m8} titer was not significantly different between primary vaccinees and revaccinees ($P=.40$). Among revaccinees, the postvaccination PRN_{LC16m8} titer in group B was marginally higher than that in group D ($P=.05$).

The percentage of primary vaccinees who seroconverted (37/41 [90.2%]) was significantly higher than that of revaccinees (93/155 [60.0%]) ($P<.001$). Among revaccinees, the percentage who seroconverted was higher in group B than in group D ($P=.002$). The geometric mean plaque-reduction neutralization titer was significantly higher among those who did not seroconvert (36.6 [95% CI, 28.0-47.8]) than among those who seroconverted (10.7 [95% CI, 8.8-13.1]) ($P<.001$).

Adverse Events

Throughout the vaccination program, no severe adverse event (eg, autoin-

Figure 2. Characteristic Skin Reaction (Take) in Vaccinia-Naive and Revaccinated Individuals 14 Days Following Vaccination With LC16m8 Vaccine

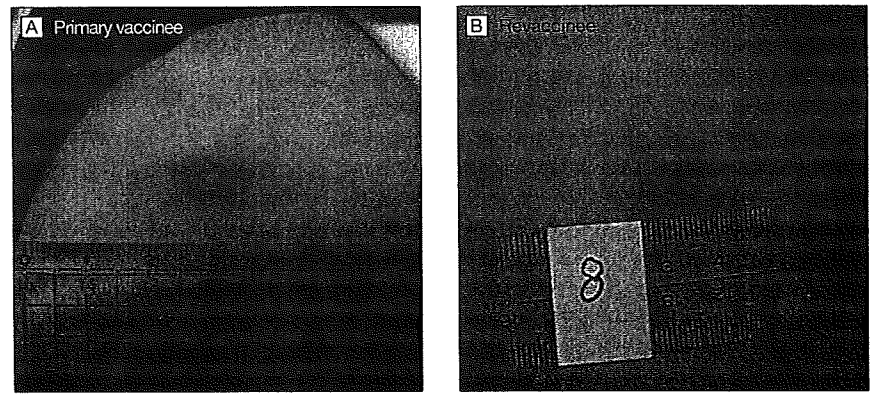

Table 3. Comparison of Prevaccination and Postvaccination Geometric Mean Titers (GMTs) and Percentage Seroconversion or Effective Boosting of Plaque-Reduction Neutralizing Titers to LC16m8 Vaccine, by Age

	GMT (95% CI)[a]				Seroconversion or Effective Boosting	
Age Group[b]	Prevaccination	*P* Value[c]	Postvaccination	*P* Value[c]	No./Total (% [95% CI])	*P* Value[d]
A (n = 41)[d]	6.1 (4.4-8.5)	<.001	112.0 (71.4-175.7)	.40	37/41 (90.2 [81.2-99.3])	<.001
B-D (n = 155)	21.0 (17.4-25.3)		137.3 (110.7-170.3)		93/155 (60.0 [52.3-67.7])	
B (n = 47)	14.4 (9.5-21.7)	.27[e]	188.2 (119.6-296.1)	.24[e]	36/47 (76.6 [64.5-88.7])	.18[e]
C (n = 45)	19.4 (13.6-27.6)	.04[f]	131.9 (88.9-195.7)	.50[f]	28/45 (62.2 [48.1-76.4])	.12[f]
D (n = 63)	29.5 (23.5-37.1)	.003[g]	111.6 (82.2-151.5)	.05[g]	29/63 (46.0 [33.7-58.3])	.002[g]

Abbreviation: CI, confidence interval.
[a] GMT calculated as probit transform of the dilution ratio of serum (no unit).
[b] Serum samples were taken from second-round vaccinees.
[c] By χ^2 test.
[d] Four individuals without vaccination take are excluded.
[e] For comparison of B and C.
[f] For comparison of C and D.
[g] For comparison of B and D.

oculation/contact inoculation, eczema vaccinatum, progressive vaccinia, generalized vaccinia, encephalitis, and symptomatic myopericarditis) was reported, and there was no need to use vaccinia immune globulin. In the 30 days after vaccination, 4 participants experienced illness thought to be consistent with an adverse event; 2 were possibly severe. One was a 26-year-old male primary vaccinee who experienced rash onset on the third day postvaccination; the rash spread from his extremities to his trunk. The patient was hospitalized 20 days after vaccination. A skin biopsy from the rash was consistent with allergic dermatitis, which did not disprove a causal relationship with vaccination. The second participant was a 29-year-old male primary vaccinee who developed a rash on his trunk 10 days postvaccination and was diagnosed with erythema multiforme. The other 2 participants were suspected of having vaccine-induced minor adverse events; one reported pain from a swollen axillary lymph node, and the other reported groin pain resulting from a bacterial infection.

No abnormal ECG findings or symptomatic heart disease were reported during the vaccination program. Three hundred forty-seven second-round vaccinees from the total 366 (94.8%) underwent assay of serum troponin T levels to assess asymptomatic myopericarditis. The distributions by age and sex in this sample were not significantly different from the whole samples ($P=.22$ and $P=.75$, respectively). Troponin T levels were below the limit of detection (0.01 ng/mL) before and after vaccination in all participants.

Among those vaccinated in the third and fourth rounds, the prevalence of minor adverse events, along with the date of onset for each event, were retrospectively reviewed using postvaccination records. In total, 491 and 575 previously unvaccinated and vaccinated individuals out of the totals of 647 (75.9%) and 592 (97.1%), respectively, were successfully monitored, resulting in a total sample of 1066 (86.0%). Participants in the third and fourth rounds had a sex distribution similar to those in the other rounds ($P=.91$) but were older ($P<.001$). No significant difference was revealed for the proportions of take (stratified by previous vaccination history) between those in the third and fourth rounds and other vaccinees ($P=.09$ for primary vaccinees, $P=.11$ for revaccinees). One hundred forty-eight minor incidents were reported, 96 (65%) of which were swelling of the axillary lymph nodes (TABLE 4). The frequency of swelling of the axillary lymph nodes was significantly smaller in revaccinees (20/575 [3.5%]) than in primary vaccinees (76/491 [15.5%]) ($P<.001$). The mean postvaccination day of onset of adverse events (swollen lymph nodes and fever) was significantly earlier in revaccinees than in primary vaccinees ($P<.001$) (TABLE 5).

Table 4. Prevalence of Adverse Events by Previous Vaccination History With LC16m8 Vaccine

Adverse Events (%)	No. of Events (%)		
	Primary Vaccinees (n = 491)	Revaccinees (n = 575)	Total (N = 1066)
Swelling of axillary lymph node	76 (15.5)	20 (3.5)	96 (9.0)
Low-grade fever (>37.5°C)	13 (2.6)	8 (1.4)	21 (2.0)
Skin itching/urticaria	4 (0.8)	3 (0.5)	7 (0.7)
Influenza-like symptom	5 (1.0)	1 (0.2)	6 (0.6)
Headache	5 (1.0)	0	5 (0.5)
Myalgia of neck, breast, upper arm	3 (0.6)	1 (0.2)	4 (0.4)
Swelling of cervical lymph node	2 (0.4)	1 (0.2)	3 (0.3)
Diarrhea	1 (0.1)	1 (0.2)	2 (0.2)
Acute sensorineural deafness	1 (0.2)	0	1 (0.1)
Dizziness	0	1 (0.2)	1 (0.1)
Swelling around orbital area	0	1 (0.2)	1 (0.1)
Arthralgia	0	1 (0.2)	1 (0.1)
Total	**110 (22.4)**	**38 (6.6)**	**148 (13.9)**

COMMENT

We evaluated the immunogenicity of LC16m8 vaccine, measuring clinical take and neutralizing antibody titer in a large-scale adult vaccination program. The immunogenicity of LC16m8 in vaccinia-naive adults was similar to that observed with the older Lister strains, and there was an adequate booster response in previously vaccinated individuals. Although the total sample size in our study limited our ability to conclusively confirm the absence of severe adverse events, no patient appeared to experience a severe

Table 5. Timing and Frequency of Low-Grade Fever (>37.5°C) and Swelling of Axillary Lymph Nodes

Event	Total	Postvaccination Day of Onset												Mean	P Value
		1	2	3	4	5	6	7	8	9	10	11	Unknown		
Low-grade fever (>37.5°C)															
Primary vaccinees	13		1	1		3	2	3	2				1	5.8	<.001
Revaccinees	8	3	2	3										2.0	
Swelling of axillary lymph node															
Primary vaccinees	76	2			6	6	12	12	7	6	2	1	22	5.6	<.001
Revaccinees	20	2	3	2	2	2	1						8	3.2	

adverse event. This finding is consistent with the concept that LC16m8 vaccine causes minimal local manifestations and systemic adverse effects.[14]

Immunogenicity of LC16m8 Vaccine

We used vaccine take and the development of neutralizing antibody titer as benchmarks of immunogenicity. The overall proportion of takes with LC16m8 appeared comparable with that seen with Lister strains in the past but, compared with Dryvax, was lower among revaccinees, which may be partly attributable to the lower proliferation property in peripheral skin (see eSupplement at http://www.jama-com). The proportion of takes among primary vaccinees did not significantly differ with age, although the numbers in all age categories other than 20 to 29 years were small, limiting statistical power. Appropriate training in vaccination technique may help achieve a higher proportion of takes, because we observed a higher proportion of takes in later vaccination rounds (Table 2). This was presumably a result of improved practice with a bifurcated needle. The improvements in take could also be observed by increasing the number of strokes given per vaccination.[25]

Another component of the take evaluation was assessment of the diameter of erythema among third-round vaccinees. We found that the diameter was greater among primary vaccinees than among revaccinees. Considering that prevaccination plaque-reduction neutralization titer was negatively associated with seroconversion, modified reactions such as smaller skin lesions and a lower proportion of takes among revaccinees could have been caused by residual immunity that prevented viral replication. Although third-round vaccinees, among whom the diameter of the local skin reaction was assessed, were older than other vaccinees, the issue of representativeness of third-round vaccinees did not influence the finding of modified reaction among revaccinees.

We evaluated the neutralizing antibody response as another measure of immunogenicity.[4,26-28] Before vaccination, plaque-reduction neutralization titers were higher in revaccinees than in primary vaccinees, suggesting that neutralizing antibody persists in individuals vaccinated more than 30 years ago, as has recently been demonstrated.[29] Such a finding may inform the duration of vaccine-induced immunity,[30] which would help determine the interval to revaccinate individuals responding first. Residual neutralizing antibody titers were also higher among individuals in the older age group, despite the time elapsed since their last vaccination. This may be because they were previously revaccinated more frequently than younger individuals, vaccinated with different vaccinia strains having different immunogenicities, or both.

After vaccination, a high percentage of seroconversion (90.2%) in primary vaccinees with clinical take was noted. Among revaccinees, higher post-vaccination plaque-reduction neutralization titer was observed among those who did not show seroconversion than among those who seroconverted, which is consistent with the literature.[31] Rather than the time elapsed since the last vaccination, our plaque-reduction neutralization titer suggests that previous vaccination with different vaccinia strains probably determined the plaque-reduction neutralization titer and seroconversion with LC16m8.

One possible limitation of this study involves the representativeness of serum samples taken from second-round vaccinees. The participants in each round were similar in terms of sex, ethnicity (Asian), and occupation (military), but the mean age of the sampled population was significantly younger in the second round than in other rounds ($P=.02$) (Table 2). Considering that previous vaccination history appeared to be a more important factor in determining seroconversion than age and that our analysis was stratified by previous vaccination history, the potential influence of previous vaccination was accounted for in our analyses of serum samples.

Plaque-reduction neutralization titer should be evaluated with caution in previously vaccinated individuals, because the titer and response can vary depending on the strain of virus used in the test. LC16m8 vaccination significantly increased the booster response of the neutralizing antibody more for LC16m8 than for Dryvax in age group B (individuals vaccinated once with the Lister strain). This may be explained by the high booster response to Lister-like epitopes of LC16m8, a response derived from the similarity of the injected LC16m8 to the immune memory resulting from the Lister vaccine. Future studies should investigate differences in the epitopes of antibodies raised by booster shots within individuals with different previous vaccinia strains. This would promote an understanding of cross-protection among orthopox virus species. Testing for plaque-reduction neutralization using variola virus would facilitate more valid and direct evaluation of immunogenicity by vaccinia immunization but is not possible in most laboratories.

Safety of LC16m8 Vaccine

We assessed serious and minor adverse reactions through participant report of symptoms suggestive of adverse events. We observed no severe adverse events. This is consistent with past studies in children (with sample size >100 000),[14] suggesting that LC16m8 would be safe in a large-scale vaccination program. The attenuated characteristics of LC16m8 and findings from preclinical studies support a higher safety profile compared with other first- and second-generation vaccines. Nevertheless, the small sample size (N=3221) in our study bears consideration. The frequency of a severe adverse event related to vaccination is believed extremely rare (<1-40 per million vaccinations[24]), such that a sample size of 124 600 individuals would be needed to ensure absence of a severe event with a 95% level of significance.